Universität Rostock

HELMHOLTZ MUNICH

JOINT MASS SPECTROMETRY CENTRE

Comprehensive Chemical Characterization of Organic Aerosols: A Complementary Approach for Health Impact Assessment

Kumulative Dissertation

zur Erlangung des akademischen Grades

doctor rerum naturalium (Dr. rer. nat.)

der Mathematisch-Naturwissenschaftlichen Fakultät

der Universität Rostock

vorgelegt von:

Elena Rosa Hartner
geb. am 31.12.1994 in Erlangen
aus München

Rostock, Oktober 2023

https://doi.org/10.18453/rosdok_id00004764

Gutachter:
Prof. Dr. Ralf Zimmermann, Universität Rostock, Lehrstuhl für Analytische Chemie
Prof. Dr. Anke Nölscher, Universität Bayreuth, Lehrstuhl für Atmosphärische Chemie

Jahr der Einreichung: 2023
Jahr der Verteidigung: 2024

Erklärung

Doktorandinnen/Doktoranden-Erklärung gemäß § 4 Absatz 1 Buchstaben g und h der Promotionsordnung der Mathematisch-Naturwissenschaftlichen Fakultät der Universität Rostock

Ich habe eine Dissertation zum Thema:

„Comprehensive Chemical Characterization of Organic Aerosols: A Complementary Approach for Health Impact Assessment"

an der Mathematisch-Naturwissenschaftlichen Fakultät der Universität Rostock angefertigt. Dabei wurde ich von **Herrn Professor Ralf Zimmermann** betreut.

Ich gebe folgende Erklärung ab:

a. Die Gelegenheit zum vorliegenden Promotionsvorhaben ist mir nicht kommerziell vermittelt worden. Insbesondere habe ich keine Organisation eingeschaltet, die gegen Entgelt Betreuerinnen/Betreuer für die Anfertigung von Dissertationen sucht oder die mir obliegenden Pflichten hinsichtlich der Prüfungsleistungen für mich ganz oder teilweise erledigt.
b. Ich versichere hiermit an Eides statt, dass ich die vorliegende Arbeit selbstständig angefertigt und ohne fremde Hilfe verfasst habe. Dazu habe ich keine außer den von mir angegebenen Hilfsmitteln und Quellen verwendet und die den benutzten Werken inhaltlich und wörtlich entnommenen Stellen habe ich als solche kenntlich gemacht.

München, den _____ _____

Elena Hartner

List of Original Publications

First Authorships

The following manuscripts were created by Elena Hartner as first author and published in peer-reviewed journals. The contribution of Elena Hartner is declared below.

Title: **On the Complementarity and Informative Value of Different Electron Ionization Mass Spectrometric Techniques for the Chemical Analysis of Secondary Organic Aerosols**

Authors: **Elena Hartner**, Andreas Paul, Uwe Käfer, Hendryk Czech, Thorsten Hohaus, Thomas Gröger, Martin Sklorz, Gert Jakobi, Jürgen Orasche, Seongho Jeong, Ramona Brejcha, Till Ziehm, Zhi-Hui Zhang, Jürgen Schnelle-Kreis, Thomas Adam, Yinon Rudich, Astrid Kiendler-Scharr, and Ralf Zimmermann

Journal: ACS Earth and Space Chemistry

Year: 2022

DOI: 10.1021/acsearthspacechem.2c00039

Elena Hartner contributed to this study by being included in its overall design and implementation. She performed the sampling, conducted the laboratory analysis of PM via TD-GC×GC-TOFMS, processed and evaluated the data, worked towards the data integration of all published chemical data and wrote and revised the manuscript.

Title: **Chemical Fingerprinting of Biomass Burning Organic Aerosols from Sugar Cane Combustion: Complementary Findings from Field and Laboratory Studies**

Authors: **Elena Hartner**, Nadine Gawlitta, Thomas Gröger, Jürgen Orasche, Hendryk Czech, Genna-Leigh Geldenhuys, Gert Jakobi, Petri Tiitta, Pasi Yli-Pirilä, Miika Kortelainen, Olli Sippula, Patricia Forbes, and Ralf Zimmermann

Journal: ACS Environmental Science and Technology

Year: 2023 (submitted)

Elena Hartner designed and implemented the majority of the chemical characterization within this study. She performed the chemical analysis of PM via TD-GC×GC-TOFMS, processed, and evaluated all chemical data and wrote the manuscript.

Co-authorship

Title: **Effects of Atmospheric Aging on Soot Particle Toxicity in Lung Cell Models at the Air-Liquid Interface: Differential Toxicological Impacts of Biogenic and Anthropogenic Secondary Organic Aerosols (SOAs)**

Authors: Svenja Offer, **Elena Hartner**, Sebastiano Di Bucchianico, Christoph Bisig, Stefanie Bauer, Jana Pantzke, Elias J. Zimmermann, Xin Cao, Stefanie Binder, Evelyn Kuhn, Anja Huber, Seongho Jeong, Uwe Käfer, Patrick Martens, Arunas Mesceriakovas, Jan Bendl, Ramona Brejcha, Angela Buchholz, Daniella Gat, Thorsten Hohaus, Narges Rastak, Gert Jakobi, Markus Kalberer, Tamara Kanashova, Yue Hu, Christoph Ogris, Annalisa Marsico, Fabian Theis, Michal Pardo, Thomas Gröger, Sebastian Oeder, Jürgen Orasche, Andreas Paul, Till Ziehm, Zhi-Hui Zhang, Thomas Adam, Olli Sippula, Martin Sklorz, Jürgen Schnelle-Kreis, Hendryk Czech, Astrid Kiendler-Scharr, Yinon Rudich, and Ralf Zimmermann

Journal: Environmental Health Perspectives

Year: 2022

DOI: 10.1289/EHP9413

Elena Hartner contributed by being included in the design and implementation of the majority of the chemical part of the study. She performed the sampling, chemical analysis, processing and evaluation of PM via TD-GC×GC-TOFMS. The corresponding section in the manuscript was written by Elena Hartner. Moreover, she worked in the process of combining biological and chemical data and was involved in the revision of the chemical results and discussion section of the manuscript.

Further Authorships

Fang, Z.; Li, C.; He, Q.; Czech, H.; Gröger, T.; Zeng, J.; Fang, H.; Xiao, S.; Pardo, M.; **Hartner, E.**; Meidan, D.; Wang, X.; Zimmermann, R.; Laskin, A.; Rudich, Y., Secondary organic aerosols produced from photochemical oxidation of secondarily evaporated biomass burning organic gases: Chemical composition, toxicity, optical properties, and climate effect. Environment International 2021, 157, 106801. DOI: 10.1016/j.envint.2021.106801

Pardo, M.; Czech, H.; Offer, S.; Sklorz, M.; Di Bucchianico, S.; **Hartner, E.**; Pantzke, J.; Kuhn, E.; Paul, A.; Ziehm, T.; Zhang, Z.-H.; Jakobi, G.; Bauer, S.; Huber, A.; Zimmermann, E. J.; Rastak, N.; Binder, S.; Brejcha, R.; Schneider, E.; Orasche, J.; Rüger, C. P.; Gröger, T.; Oeder, S.; Schnelle-Kreis, J.; Hohaus, T.; Kalberer, M.; Sippula, O.; Kiendler-Scharr, A.; Zimmermann, R.; Rudich, Y., Atmospheric aging increases the cytotoxicity of bare soot particles in BEAS-2B lung cells. Aerosol Science and Technology 2023, 1-17. DOI: 10.1080/02786826.2023.2178878

Pardo, M.; Offer, S.; **Hartner, E.**; Di Bucchianico, S.; Bisig, C.; Bauer, S.; Pantzke, J.; Zimmermann, E. J.; Cao, X.; Binder, S.; Kuhn, E.; Huber, A.; Jeong, S.; Käfer, U.; Schneider, E.; Mesceriakovas, A.; Bendl, J.; Brejcha, R.; Buchholz, A.; Gat, D.; Hohaus, T.; Rastak, N.; Karg, E.; Jakobi, G.; Kalberer, M.; Kanashova, T.; Hu, Y.; Ogris, C.; Marsico, A.; Theis, F.; Shalit, T.; Gröger, T.; Rüger, C. P.; Oeder, S.; Orasche, J.; Paul, A.; Ziehm, T.; Zhang, Z.-H.; Adam, T.; Sippula, O.; Sklorz, M.; Schnelle-Kreis, J.; Czech, H.; Kiendler-Scharr, A.; Zimmermann, R.; Rudich, Y., Exposure to naphthalene and β-pinene-derived secondary organic aerosol induced divergent changes in transcript levels of BEAS-2B cells. Environment International 2022, 166, 107366. DOI: 10.1016/j.envint.2022.107366

Zhang, Z. H.; **Hartner, E.**; Utinger, B.; Gfeller, B.; Paul, A.; Sklorz, M.; Czech, H.; Yang, B. X.; Su, X. Y.; Jakobi, G.; Orasche, J.; Schnelle-Kreis, J.; Jeong, S.; Gröger, T.; Pardo, M.; Hohaus, T.; Adam, T.; Kiendler-Scharr, A.; Rudich, Y.; Zimmermann, R.; Kalberer, M., Are reactive oxygen species (ROS) a suitable metric to predict toxicity of carbonaceous aerosol particles? Atmos. Chem. Phys. 2022, 22 (3), 1793-1809. DOI: 10.5194/acp-22-1793-2022

Acknowledgements

I would like to extend my sincere thanks to Prof. Dr. Ralf Zimmermann for his support and supervision and for giving me the opportunity and framework to work as a PhD student in his group.

Furthermore, I am especially grateful for the continuous support from my supervisor, Thomas Gröger. Thank you so much for your dedication, advice, patience and most of all for your care and encouragement in the demanding periods of the past years. Tom, I could not have undertaken this journey without you.

I also wish to thank Dr. Jürgen Orasche and Dr. Hendryk Czech for their valuable guidance in realizing my studies, their scientific support and for teaching me so much about aerosols.

Many thanks to Prof. Dr. Andreas Held for first awakening my interest in aerosol science during my bachelor studies and for supporting me as a member of my PhD thesis committee throughout these past four years.

I further would like to acknowledge all the national and international cooperation partners for their support and pleasant collaboration. It's been a great experience to work with you in an interdisciplinary and international team.

Furthermore, I would like to thank all my colleagues with whom I have worked closely on various projects, studies, and campaigns. Special thanks to Dr. Uwe Käfer, Dr. Svenja Offer, Andreas Paul, Dr. Nadine Gawlitta, Ramona Brejcha, Lukas Schwalb, Dr. Barbara Giocastro and Dr. Martin Sklorz!

Moreover, my heartfelt thank you goes to all my wonderful colleagues at CMA for making the past four years so much more enjoyable. I am grateful for your helpfulness, interesting conversations and discussions, assistance in the lab, encouraging words, fun lunch and coffee breaks, and memorable evenings inside and outside of CMA. Most of all, I would like to thank Jana, Svenja and Ramona for their unwavering personal support during the most challenging times, for their enthusiasm and kindness, and for always putting a smile on my face.

Last but not least, I would like to thank my husband Simon, who has always stood by me no matter what, and on whom I have been able to rely completely as we embarked on our PhD journeys together. I also am forever grateful for my parents and my sister Mona for their unconditional love and support and for being there for me every step of the way.

This study was financially supported by the Helmholtz International Laboratory *aeroHEALTH* (https://www.aerohealth.eu), which is gratefully acknowledged.

Zusammenfassung

Luftverschmutzung durch atmosphärische Aerosole ist eines der größten umweltbedingten Gesundheitsrisiken und ist weltweit für Millionen von vorzeitigen Todesfällen und verlorenen Lebensjahren durch Gesundsheitseinschränkungen verantwortlich. Atmosphärische Aerosole werden entweder direkt aus natürlichen und anthropogenen Quellen emittiert oder sekundär durch atmosphärische Prozesse gebildet und durch Oxidationsprozesse verändert. In jedem Fall kann der chemische Fingerabdruck von Aerosolen eine Vielzahl unterschiedlicher organischer Verbindungen umfassen, die Auswirkungen auf die menschliche Gesundheit, das Klima und die Umwelt haben.

Für diese Arbeit wurden sowohl Aerosole aus kontrollierten Simulationen, die im Labormaßstab aus Naphthalin- und ß-Pinen-Vorläufergasen aufgebaut wurden, als auch Aerosole aus realen Emissionen der Biomasseverbrennung, die im Feldversuch durchgeführt wurden, hinsichtlich ihrer physikalischen, chemischen und biologischen Parameter untersucht. Es wird ein analytischer Ansatz mit verschiedenen Online- und Offline-Methoden für eine umfassende chemische Analyse organischer Aerosolpartikel vorgestellt. Einen Schwerpunkt stellt die Kombination verschiedener auf Elektronenionisation und Flugzeitmassenspektrometrie basierender Massenspektrometer dar.

Um detaillierte molekulare Informationen über diese hochkomplexen organischen Gemische aus frischen und gealtertern Aerosolen zu erhalten, wurde die zweidimensionale Gaschromatographie (GC×GC) mit thermischer Desorption und Flugzeitmassenspektrometrie kombiniert. Dabei wurden einzelne chemische Spezies identifiziert und hinsichtlich ihres Oxidationsgrades und ihrer chemischen Klassenzugehörigkeit untersucht. Dies ermöglichte Aussagen über die Zusammensetzung der Aerosole, deren Veränderung durch photochemische Oxidation und über spezifische Emissionsmarkerverbindungen. Darüber hinaus wurden ein hochauflösendes Massenspektrometer mit Direkteinlasssonde und ein Aerosol-Massenspektrometer eingesetzt, um Verbindungen mit höherem Molekulargewicht zu untersuchen, die nicht mittels Gaschromatographie untersucht werden konnten. Auf diese Weise konnte eine große Bandbreite an Analyten in Bezug auf Flüchtigkeit und Polarität untersucht werden. Diese interdisziplinäre Studie konnte zeigen, dass sich die atmosphärische Chemie erheblich auf die chemische Zusammensetzung von organischen Aerosolen auswirkt, was sich auch in deren gesundheitsschädigenden Wirkung widerspiegelt.

Ausgehend von Untersuchungen einzelner Vorläufergase für die sekundäre Aerosolbildung umfasst diese Arbeit zudem eine Fallstudie zur Biomasseverbrennung von Zuckerrohr, bei der Emissionen aus der Verbrennung im Feld und in kontrollierter Laborumgebung analysiert wurden. Dabei wurden die GC×GC Daten der analysierten Labor- und Feldproben mit gerichteter und ungerichteter Datenauswertemethoden verglichen. Die Ergebnisse zeigen erhebliche Unterschiede zwischen den durchgeführten Feldexperimenten und den Laborsimulationen auf, welche im Hinblick auf die

unterschiedlichen Verbrennungsbedingungen, Brennstoffzusammensetzungen und atmosphärische Oxidation diskutiert werden.

Diese Arbeit leistet einen wertvollen Beitrag zum Verständnis des Zusammenhangs zwischen der toxikologischen Wirkung von Aerosolen und ihrer chemischen Zusammensetzung, aber auch der Abhängigkeit der chemischen Zusammensetzung vom experimentellen Aufbau. Die Bewertung der Komplexität atmosphärischer organischer Aerosole erfordert einen umfassenden Forschungsansatz, der sowohl Labor- als auch Feldstudien integriert und eine Vielzahl analytischer Instrumente einsetzt.

Abstract

Air pollution from atmospheric aerosols is one of the greatest environmental health risks, causing millions of deaths and years of healthy life lost worldwide. Atmospheric aerosols comprise a wide variety of organic compounds, either directly emitted from natural or anthropogenic sources, or produced and altered by secondary atmospheric processes. Either way, the chemical fingerprint may encompass thousands of compounds that affect human health, climate and the environment.

For this thesis, both laboratory-produced aerosols (derived from naphthalene and ß-pinene precursor gases) and atmospheric aerosols from real-world biomass combustion emissions have been characterized for their physical, chemical and biological parameters using online and offline methods. This thesis combines state-of-the-art and novel instrumentation based on electron ionization (EI) and time of-flight mass spectrometry (TOFMS) to propose an analytical scenario for a comprehensive chemical analysis of the organic fraction in PM.

A thermal desorption (TD) two-dimensional gas chromatography (GC×GC) TOFMS technique was used for the molecular analysis of the particle-bound vaporizable organic species of fresh and aged aerosols to understand their chemical composition, changes with aging, and specific emission marker compounds. This involved comparing individual chemical species, assessing their degree of oxidation, and categorizing chemical classes. In addition, atline direct inlet probe and online aerosol mass spectrometry were applied to study higher molecular weight compounds inaccessible by gas chromatography. This allowed a wide range of analytes to be analyzed with respect to volatility and polarity, thereby extending the total mass of PM accessible to EI–TOFMS. This interdisciplinary study showed that the chemical composition of PM is significantly influenced by atmospheric chemistry, with important implications for its adverse health effects.

Moving on from aerosol systems derived from individual secondary organic aerosol precursor gases, this thesis further encompasses a case study about open-field burning experiments and controlled combustion laboratory studies of sugar cane biomass. In these investigations, we compare the GC×GC chemical profiles for each experimental type using targeted and non-targeted evaluation approaches. The outcomes of our study revealed substantial differences between the conducted field experiments and laboratory simulations. These observed variations between field and laboratory experiments are discussed in terms of disparities in combustion conditions, fuel composition and atmospheric oxidation.

This thesis makes a valuable contribution to understanding the relationship between the toxicological effects of aerosols and their chemical composition, but also the dependence of the chemical composition on the experimental setup. Assessing the complexity of atmospheric organic aerosols requires a comprehensive research approach which integrates both laboratory and field investigations and uses different analytical toolsets.

Table of Contents

1 Motivation

Atmospheric aerosols are ubiquitous [1] and have a significant impact on the environment, climate, and health [2]. Worldwide exposure to particulate matter (PM) contributed to over 6 million premature deaths in the year 2019 [3]. The sources of aerosols are extremely diverse, but can broadly be classified as natural and anthropogenic. In addition to their origin, the chemical and physical composition of atmospheric aerosols is very heterogeneous and complex, and this complexity is further increased by atmospheric chemistry processes in the atmosphere [4]. As a result of the heterogeneous sources, formation and evolution pathways of aerosols, they encompass a broad range of sizes, chemical compositions, and morphological characteristics [5].

This complex mixture of aerosols with different physical and chemical properties is an essential part of the human environment, as we are exposed to them on a daily basis. However, their complexity makes it difficult to establish clear cause-effect relationships, since both biological interactions relevant to health and the physicochemical processes in the atmosphere are extremely complex and interact with each other. As such, a comprehensive physicochemical characterization of aerosols to unravel their sources, evolution processes and biological responses is imperative to fully understand the effects they induce within this wide spectrum of relevant fields.

However, this is a significant challenge, as most analytical methods are generally tailored to focus on a specific analyte or group of analytes [6]. In contrast, each particle consists of numerous (organic) compounds, for which a complete description is not possible with the available analytical toolsets. For this reason, it is necessary to single out some aspects and to describe them as comprehensively as possible. Therefore, this dissertation presents the complementary utilization of analytical techniques, applicable to both laboratory and field studies, aiming to comprehensively enhance our comprehension of the impact of the semi-volatile organic fraction of atmospheric aerosols on human health.

2 Introduction

This thesis was conducted between August 2019 and September 2023 within the framework of the Helmholtz International Laboratory *aeroHEALTH* research project (https://www.aerohealth.eu), which aims to establish a direct link between emission scenarios, chemical composition, atmospheric oxidation, and health effects of complex aerosols. Within this multidisciplinary project, in addition to the toxicological and physical characterization of the aerosol, a comprehensive chemical characterization was carried out, which is the fundamental subject of the thesis presented here.

2.1 Sources and Implications of Atmospheric Aerosols

Atmospheric aerosols originate from both anthropogenic and natural sources. The diverse sources of atmospheric aerosols are exemplary shown in (**Figure 1**). Natural sources include emissions from the ocean, soil, vegetation, wildfires and volcanic activity [7]. Since the onset of industrialization, anthropogenic sources have become the greatest contributor to air pollution by PM, notably through the combustion of fossil fuels (e.g. coal, oil) or biofuels (e.g. wood, vegetable oils, peat) [8]. In addition, human-caused vegetation fires, industrial processes, agriculture, transportation, heating and domestic activities are significant contributors to aerosol production [9].

Atmospheric aerosols have a significant impact on various aspects of our environment (**Figure 1**). Aerosols directly affect the Earth's climate through scattering, absorbing, and emitting electromagnetic radiation at different wavelengths. Moreover, they have an indirect climatic effect by serving as cloud condensation nuclei (CCN) and influencing properties and lifetime of clouds [10]. They further are a major concern for visibility and human health. According to the World Health Organization (WHO), the majority of the global population (~ 99%) is exposed to air surpassing WHO guideline limits and containing high levels of pollutants, resulting in millions of deaths every year and comprised years of healthy life [8]. Air pollution poses a risk factor for a great range of different diseases, which includes respiratory issues such as asthma, bronchiolitis, lung cancer and chronic obstructive pulmonary disease (COPD), but further also adversely affects human health by causing diseases of the cardiovascular, dermal, and central nervous system [2, 11, 12]. Finally, atmospheric aerosols also play an important role in atmospheric chemistry. On the one hand, the high oxidative potential of the atmosphere, determined by oxidants such as ozone (O_3), hydroxyl radicals ($OH\bullet$) or nitrate radicals ($NO_3\bullet$), is an important contributor to the production of secondary organic aerosols (SOA) from gaseous precursors [10]. Conversely, atmospheric aerosols themselves also play a significant role in oxidation reactions in the atmosphere [13].

2.2 General Terminology and Classification of Atmospheric Aerosols

Aerosols are defined as a suspension of solids and liquids in a gaseous medium [14]. The terminology of aerosols is quite complex, given the great diversity of aerosol sources, formation pathways, chemical compositions, phases, sizes and morphologies.

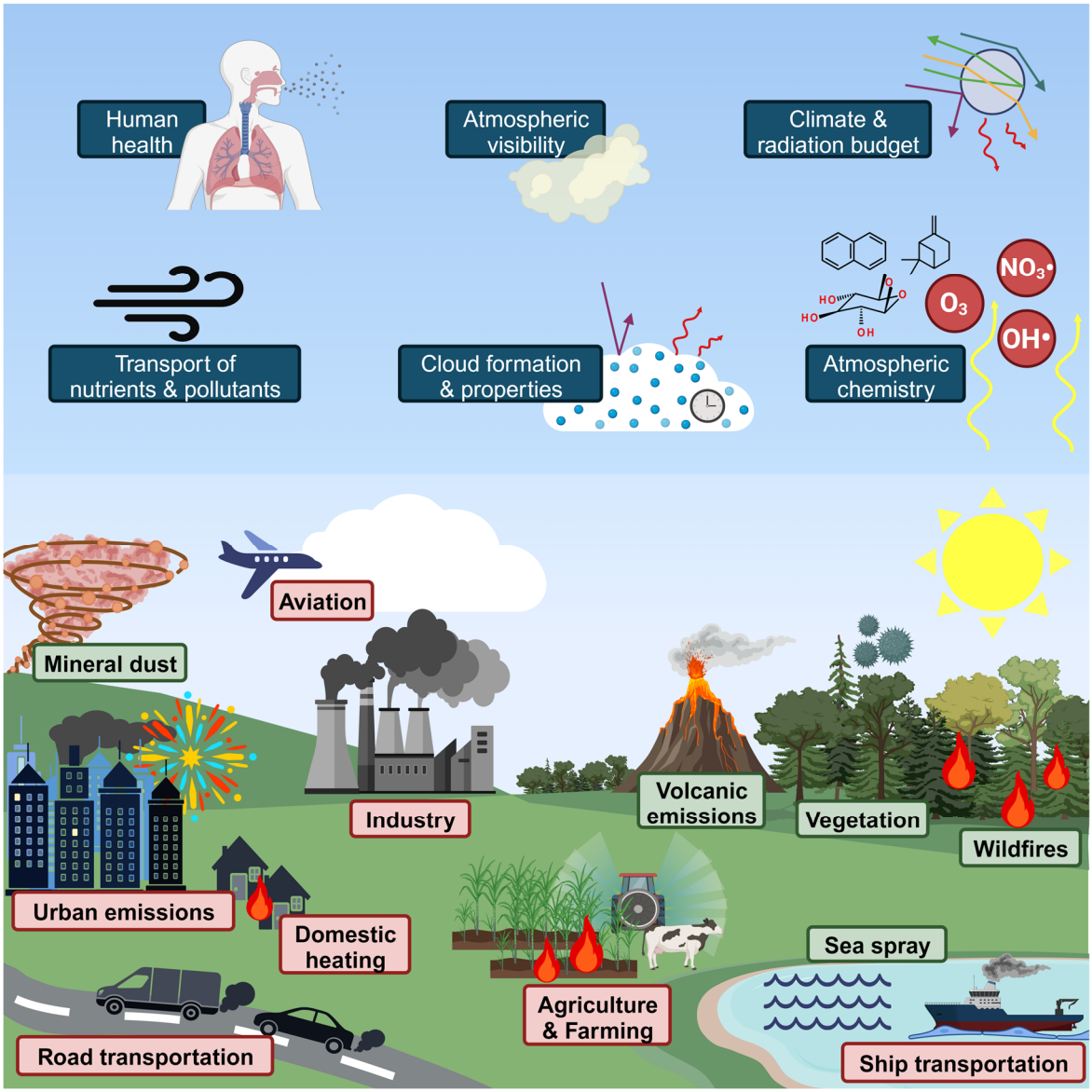

Figure 1: *Emission sources of atmospheric aerosols (bottom). Anthropogenic sources (red), amongst others, include motorized transportation on land, sea and air; industry (e.g. combustion of fossil fuels); agriculture; farming; biomass burning; as well as domestic housing and heating. Natural sources (green) of atmospheric aerosols, amongst others, include wildfires; sea spray; volcanic activities; vegetation (aerosol precursor gases, pollen, spores, bacteria); and mineral dust. Implications and relevance of atmospheric aerosols (top). Aerosols influence the Earth's climate and the atmospheric radiation budget (direct climate effect); cloud formation and cloud properties (indirect climate effect); atmospheric visibility; transport of nutrients and pollutants; human health; and atmospheric chemistry. Created with BioRender.com.*

A general way of categorizing aerosols is by their size. Particulate matter (PM), which refers only to the suspended particles (liquid droplets or solids) as part of the aerosol, can be classified by their size into coarse (10 µm), fine (2.5 µm) and ultrafine (0.1 µm) particles based on their aerodynamic diameter [14], which is the diameter of a spheric particle with unit density having the same motion characteristics in air as the particle of interest [15]. The term PM is commonly defined as PM_d for the fraction of PM with an aerodynamic diameter of d µm or less. For example, PM_{10} refers to all

PM with a diameter of 10 µm or less, which is the inhalable particle-bound fraction of aerosols. $PM_{0.1}$ refers to the ultrafine particle (UFP) fraction, which are of particular health concern due to their ability to reach the most peripheral regions of the lung [16].

Furthermore, aerosols can generally be categorized as either primary aerosols, which originate directly from diverse sources (e.g. biomass burning, fossil fuel combustion, volcanic events, mineral dust, or biological material), or secondary aerosols, which are formed as a result of gas-to-particle conversion processes in the atmosphere [17]. This will be discussed in more detail in the following.

Finally, atmospheric aerosols can be classified according to their inorganic and organic fractions. The most abundant ions present in inorganic aerosols are sulfate (SO_4^{2-}), ammonium (NH_4^+) and nitrate (NO_3^-) or their mixtures [9]. Organic aerosols (OA) constitute a significant fraction of the tropospheric particulate mass, ranging from 20% to 90% [18]. When elemental carbon (EC) or black carbon (BC) is included, the term carbonaceous aerosol is used. EC is chemically inert refractory material, which is exclusively emitted from incomplete combustion processes [19], whereas OA can be either primarily emitted or secondarily formed, in which case they are defined as primary organic aerosol (POA) and secondary organic aerosol (SOA), respectively [18]. Depending on their volatility (vapor pressure), which is the most important parameter influencing the partitioning of molecules between gas and particle phases, OAs are classified as either gaseous volatile organic compounds (VOCs), semi-volatile organic compounds (SVOCs), or non-volatile organic compounds (NVOCs) [10]. Among the NVOCs are so called extremely low volatility organic compounds (ELVOCs), which often are highly functionalized oligomeric species attached to the aerosol surfaces [20].

Within the framework of this thesis, the focus lies on the semi-volatile organic fraction of both POA and SOA of different matrices and of different origin.

2.3 Formation of Secondary Organic Aerosols (SOA) and Atmospheric Aging

Gaseous VOCs and POAs are directly released into the atmosphere from both biogenic and anthropogenic sources. VOCs are essential components of tropospheric chemistry due to their potential to undergo oxidation, leading to the formation of less volatile products, known as SVOCs and NVOCs. These transformed compounds can then partition into the particulate phase and contribute to the formation of SOA. Notable oxidizing agents in the atmosphere include hydroxyl radicals, ozone, and nitrate radicals. Freshly formed POA and SOA can undergo subsequent oxidation and atmospheric processing, resulting in the production of aged organic aerosols [10]. Atmospheric oxidation leads to the formation of carbon-oxygen and cleavage of carbon-hydrogen bonds, as a result of functionalization and fragmentation reactions [21, 22]. This results in the incorporation of polar functional groups into the carbon backbone of OA [23].

Figure 2 A illustrates the processes involved in the generation of SOAs and their subsequent aging in the atmosphere. The partitioning of aerosols between the gas and particulate phase depends on their liquid- or solid-phase vapor pressures (v_p) and further on factors such as their solubility in water

and whether they are pure substances or mixtures of compounds. Most atmospheric emissions of organic compounds occur as gaseous VOCs and tend to have high vapor pressures. However, as oxidation in the atmosphere progresses, starting with the formation of carbonyls and esters, the vapor pressure decreases, as the polarity increases. Further oxidation to alcohols and carboxylic acids leads to reduced vapor pressures due to hydrogen bonding. This trend intensifies for compounds with multiple functionalities like diols and dicarboxylic acids, resulting in even lower vapor pressures. For instance, the partitioning tendency shifts towards the aerosol phase for n-alkanes with more than 20 carbon atoms, in contrast to dicarboxylic acids with only at least 3 carbon atoms. [24]

The transition of a compound from the gaseous phase to the particulate phase can occur by either new particle formation processes (nucleation) or particle alteration (condensation and sorption) (**Figure 2 B**). Nucleation occurs when vapor concentrations are particularly high, causing the vapor itself to initiate the phase change, resulting in an uniform phase. When there are existing surfaces (such as solid-phase soot particles) clusters of condensed, adsorbed and absorbed molecules can form on these surfaces. [25]

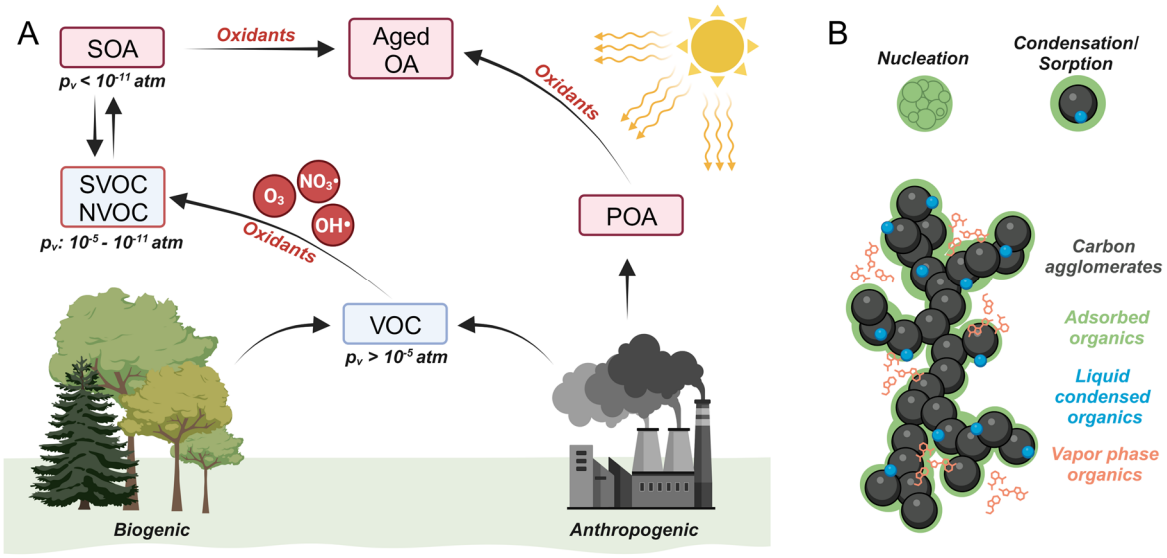

Figure 2: A) *Emissions of POAs and VOCs from biogenic and anthropogenic sources and the formation of SOA through oxidation processes in the atmosphere. The illustration shows the transitions between gas- and particle-phase organic compounds. Major oxidants in the atmosphere are hydroxyl and nitrate radicals, as well as ozone. Gas-phase species are shown in blue, particle-phase species in red. The illustration was adapted from [10]. Provided vapor pressures (p_v) at ambient temperature were taken from [24].* ***B)*** *Diagram showing gas-to-particle conversion processes through nucleation and condensation/sorption (top). Schematic representation showing carbon agglomerates serving as sorption and condensation seed particle for (oxygenated) organic compounds (bottom). Adapted from [26, 27]. Created with BioRender.com.*

2.4 Chemical Composition of Organic Aerosols

OAs comprise a vast array of chemical constituents. For instance, two-dimensional gas chromatography measurements have revealed over 10,000 individual organic components, ranging from alkanes to poly-oxygenated organic species [28]. OAs constituents belong to different classes

of organic compounds, encompassing (multi-functional) aromatic and aliphatic compounds. This includes polycyclic aromatic hydrocarbons (PAHs), monosaccharides, alkanoic acids, nitro- and oxy-PAHs, as well as aliphatic alcohols, carbonyls, and carboxylic acids [7, 17, 29]. Within these groups, many compounds are acknowledged for their biological toxicity (see **section 2.5**).

2.4.1 Biogenic VOC Precursors for SOA

As VOCs degrade in the atmosphere, they produce a variety of multifunctional organic compounds. Their high chemical diversity and different oxidation pathways have a significant impact on the chemical composition of SOA [30, 31]. Most biogenic VOCs are very reactive in the troposphere with atmospheric lifetimes between minutes and hours [32] and originate mainly from terrestrial ecosystems with vegetation contributing the highest emission rates [33]. However, there are also important BVOC emissions from the oceans [4]. The main classes of biogenic VOCs are isoprene, monoterpenes (e.g. α-pinene, β-pinene, limonene) and sesquiterpenes. Isoprene accounts for approximately 50% of the VOC budget [32], followed by monoterpenes (16%) [34]. Other biogenic VOCs include acetaldehyde and formaldehyde, and less reactive compounds such as methanol, acetone and formic acid [33].

α- and β-pinene are the two isomers of pinene (class of monoterpenes) and are emitted mainly by coniferous trees. They have similar structures but differ in the position of their double bond, which is endocyclic in α-pinene and exocyclic in β-pinene (**Figure 3**). Oxidation reactions are initiated by OH attack on the double bond. The major oxidation product of α-pinene is pinonaldehyde and of β-pinene is nopinone [34].

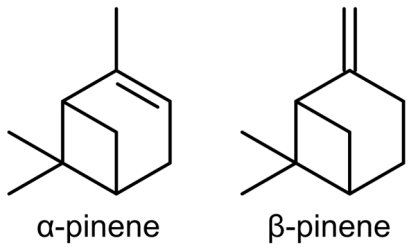

Figure 3: *Chemical structure of both pinene isomers, α-pinene and β-pinene*

2.4.2 Anthropogenic VOC Precursors for SOA

On a global scale, VOCs released from natural sources exceed those from human activities by a factor of ~10. In urban environments, however, anthropogenic VOCs greatly exceed biogenic VOCs and are typically composed of ~45% alkanes, ~10% alkenes, ~20% aromatic hydrocarbons ~ 15% oxygenated compounds. [35]

Although the distinction between anthropogenic and biogenic VOCs is somewhat arbitrary from a chemical perspective (the same compounds are often emitted by both anthropogenic and biogenic sources), aromatic hydrocarbons such as e.g. benzene, toluene and PAHs are considered to be typical and abundant anthropogenic emissions resulting from a wide range of human activities [36]. PAHs are organic compounds consisting of at least two fused aromatic ring structures and originate mainly from the incomplete combustion of organic fuels. While larger PAHs are predominantly present in the particulate phase, 2- to 4-ring PAHs exist mainly in the gas phase with impact on gas phase atmospheric chemistry [37]. As such, aromatic hydrocarbons have been demonstrated to have a

substantial impact on the generation of SOA in urban areas [38]. Furthermore, PAHs are well known as toxic, mutagenic and carcinogenic [2, 39].

2.4.3 Biomass Burning Aerosols

Biomass burning (from both natural and anthropogenic sources such as wildfires, agricultural fires, biofuel combustion) is one of the largest sources of emissions of POA, various trace gases and BC to the global atmosphere [40-43]. Anthropogenic emissions that contribute significantly to global biomass burning include the burning of biofuels (wood, charcoal, agricultural waste) and the burning of crop residues in open fields [44]. Agricultural fires are a widely used strategy around the world for a variety of purposes, including waste management (e.g. clearing agricultural land for cultivation), pest and disease control, and pre-harvest removal of excess agricultural trash [45].

Emissions from agricultural fires are highly variable depending on the biomass composition and combustion properties [46]. Under ideal combustion conditions, which are seldom achieved, all organic emissions would be oxidized to form oxygen and water. Instead, biomass burning emissions are thermal decomposition products originating from the biomass used as fuel.

A substantial part of the terrestrial biomass is composed of lignocellulosic biomass, which encompasses hardwoods, conifers, and a variety of energy and food crops such as sugarcane, rice, cotton, maize, and wheat [47]. The primary constituents of lignocellulosic biomass consist of cellulose, hemicellulose, and lignin, which are interconnected in the plant's cell wall (**Figure 4**). Cellulose is a carbohydrate polymer composed of repeating glucose units wrapped by the dense structure of hemicellulose, which are branched polymers of pentose and hexose sugars. Lignin, a heteropolymer of phenolic compounds (p-coumaryl alcohol, coniferyl alcohol, sinapyl alcohol), binds to the hemicellulose through electrostatic interactions. [48, 49]

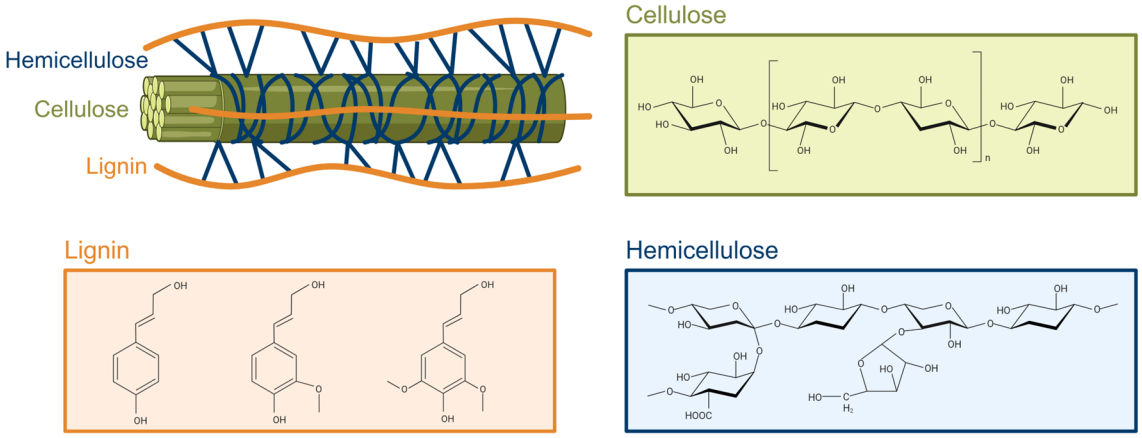

Figure 4: *Structural organization of the cell wall of lignocellulosic biomass composed of cellulose, hemicellulose, and lignin, approximately in a ratio of 4:3:3 [49]. The lignin monomers shown from left to right are p-coumaryl alcohol, coniferyl alcohol and sinapyl alcohol. Created with BioRender.com.*

POA emissions from biomass combustion include compounds of several chemical classes, including PAHs, n-alkanes, n-alkenes, n-alkanoic acids, n-alkanols, as well as derivatives of monosaccharides from cellulose pyrolysis, methoxyphenols from lignin pyrolysis, and biomarkers such as steroids and terpenoids [50]. The primary organic combustion product from biomass combustion is the anhydrous sugar levoglucosan, which is formed by the thermal decomposition of cellulose. Levoglucosan, together with the organic tracers mentioned above, serves as a widely used marker compound for biomass burning emissions. However, additional tracers are required for the source apportionment of biomass-specific combustion emissions.

2.5 Health Impact of Aerosols

Airborne particles have been associated with both local and systemic adverse health effects, including respiratory diseases, cardiovascular diseases, reproductive abnormalities, and neurodegenerative diseases [7]. The size of the particles (described as their aerodynamic diameter) is an important factor in how deeply they penetrate and are deposited in the lungs [51] (**Figure 5**). The predominant mechanisms by which PM is deposited in the respiratory system include impaction, sedimentation, interception, and diffusion [52]. While larger particles are usually cleared by the body's defense mechanisms in the upper airways, smaller particles ($PM_{2.5}$) are retained in the respiratory system. Furthermore, particles with diameters below ~0.5 µm are not only confined to the bronchioles or the surface of the alveoli, but are able to cross the blood-gas barrier and accumulate in organs beyond the lungs (e.g. liver, kidneys) [53]. In addition to particle size, further physical properties, such as mass, shape, surface and morphology, and chemical composition of both the particulate and the gas phase compounds may contribute to the biological responses within and beyond the respiratory system. However, the exact mechanisms underlying these health effects are still not fully understood [54] and are the subject of current research.

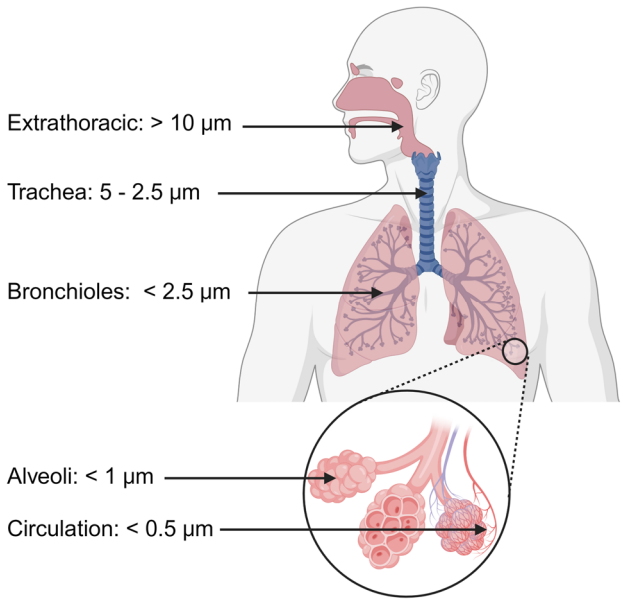

Figure 5: *Schematic of the human respiratory tract showing the size-dependent deposition of inhaled particles in different regions of the lung. Created with BioRender.com.*

2.6 Laboratory and Field Experiments in Aerosol Science

Aerosol studies encompass both field and laboratory experiments to unravel the complex processes that govern aerosol formation and evolution. By characterizing aerosols in their natural environment, field measurements can provide real-world insights. For example, biomass burning is a highly variable process, where emissions depend on several complex factors, such as e.g. fuel composition,

moisture content, combustion and weather conditions, dilution with air, fire temperature and background OA concentrations [41, 55, 56]. Field campaigns are therefore necessary to capture the realistic formation and natural evolution of emissions, but uncontrolled and highly variable field conditions can limit the scope of field experiments and make data interpretation difficult.

In contrast, laboratory experiments provide control over environmental and chemical conditions, which allows for the systematic analysis of factors that influence aerosol formation, aging and transformation. This enables the study of specific variables, albeit with the challenge of replicating the complexity of the atmosphere [57]. While field observations show that aerosols vary greatly in terms of size, morphology, physical and chemical properties, laboratory experiments greatly simplify this complexity. For example, single-component model systems are often applied as surrogate mixtures [6]. Nonetheless, the investigation of simplified systems under laboratory settings can considerably enhance our knowledge of the chemical and physical properties of primary and secondary emissions [58]. Laboratory experiments mainly use smog chambers or flow tube reactors, both of which allow the aging and transformation of aerosols to be studied under different conditions (temperature, humidity, oxidants, light intensity and sources, time scales) [58]. Smog chambers with sizes up to ~270 m^3 simulate atmospheric aging on the order of hours to days. On the other hand, oxidation flow reactors (OFR) with smaller sizes up to ~1 m^3 subject aerosols to higher degrees of aging in shorter time scales and at higher concentrations of atmospheric oxidants [58].

One commonly used flow tube is the Potential Aerosol Mass (PAM) OFR, which holds ~19 L and operates with continuous air flow, ultraviolet (UV) light sources (185 nm and 254 nm) and short residence times. The reactive gases O_3, $OH\bullet$, and HO_2 are produced directly inside the PAM chamber by irradiation of humidified, purified air at 185 nm to produce $OH\bullet$ and HO_2 from H_2O, as well as O_3 from O_2. Furthermore, the photolysis of O_3 at 254 nm generates singlet oxygen $O(^1D)$, which reacts with water vapor to form $OH\bullet$. [59]

Bridging the gap between field and laboratory experiments, and effectively integrating their different aspects, is a major challenge [6]. However, such integration has the potential to greatly contribute to a comprehensive understanding of aerosol formation, aging, and transformation, and to facilitate the identification of molecular markers for source apportionment [57, 60].

2.7 Analytical Chemistry of Organic Aerosols

According to Goldstein and Galbally [24] there are approximately 100 possible isomers for alkanes with a carbon number of 10. This number increases to over 1 million when additionally considering typical heteroatoms and substitutions. Given the possibility that many of these compounds are present in the atmosphere, and the consequent overwhelming number of individual compounds present in organic aerosols, their complete chemical characterization presents an analytical challenge. Instrumentation for chemical characterization and quantification can broadly be categorized into offline and online techniques.

Among the most common spectroscopic approaches, used for aerosol chemical characterization are nuclear magnetic resonance (NMR) and infrared (IR) spectroscopy [4]. However, state-of-the-art techniques for the chemical characterization of complex mixtures of organic aerosols on the molecular level are typically mass spectrometric (MS) approaches. The combination of high sensitivity and molecular specificity makes MS particularly useful for molecular analyses. Mass spectrometric determination of elemental formulas for ions within the spectrum is achieved by accurate mass measurements at the parts per million (ppm) level. Concentrations of organic PM in the atmosphere are typically in the range of 1-10 μg m^{-3}, whereas the concentrations of individual compounds can be in the range of pg m^{-3} to ng m^{-3}. Therefore, the ability to quantify small amounts of individual molecular species (in the low ng range) is crucial for aerosol analytics and is effectively fulfilled by techniques such as gas chromatography mass spectrometry (GC–MS) or liquid chromatography mass spectrometry (LC–MS). [10]

While these offline techniques provide molecular information on individual chemical species or functional groups in OA, they typically require large amounts of sample material, typically collected via absorption, filtration, or impaction, which results in a low time resolution. GC–MS approaches typically use electron ionization (EI) for organic mass spectrometry due to its high ionization efficiency and reproducible fragmentation. In contrast, “soft” ionization techniques include chemical ionization (CI), electrospray ionization (ESI) and photoionization (PI), which result in a limited degree of analyte fragmentation, higher selectivity and often preserve the molecular ion.

As an additional tool for accurate mass measurements, Fourier transform ion cyclotron resonance MS (FTICRMS), with its ultra-high mass resolution (>100,000), allows the determination of the molecular composition even at higher masses, as is the case for oligomeric species in aerosols [61-63]. Although not typically applied for aerosol samples, another MS technique for the chemical characterization of high boiling samples is direct inlet probe (DIP) high resolution MS [64, 65].

Online methods have the benefit of providing highly time-resolved, real-time data to map the dynamics of a process, but typically provide less specific information about the chemical composition of individual species. Examples for online techniques for aerosol characterization are aerosol mass spectrometers (AMS) for the quantitative speciation of nonrefractory compounds in size-segregated particle fractions [66-68] and single particle mass spectrometers (SPMS), which stand out for characterizing the chemical loading of individual particles [69, 70]. For the detection of gas phase constituents, techniques, such as proton transfer reaction mass spectrometry (PTR-MS) [71, 72] and photoionization mass spectrometry (PIMS), which allows for a soft and sensitive ionization of organic constituents [73] are applied.

As a result, offline and online techniques are not mutually exclusive, but are complementary to each other. Consequently, a combination of different MS systems is required for a complete characterization of the OA.

3 Scope of the Thesis

The multiple emission sources and oxidation pathways of organic aerosols contribute to their wide range of physicochemical characteristics, including molecular size, volatility, degree of oxidation and functional groups [5]. The characterization of such a large number of extremely diverse compounds presents a major challenge for aerosol analytics, which has the overarching demanding objective of building bridges to various other disciplines of aerosol research. According to Galvão *et al.* [74], there are three primary motivations for studies on the physicochemical characterization of aerosols: (a) elucidating the source, formation pathways reactivity and fate of atmospheric aerosols; (b) assessing the impact of atmospheric aerosols on human heath; and (c) evaluating and enhancing analytical methods and their applications. Moreover, there are three different scientific approaches, which are commonly applied to study atmospheric aerosols [6]: (A) laboratory studies of model systems simulating atmospheric aerosols; (B) field measurements; and (C) modeling analysis.

The motivation and scope of this thesis results from a combination of these aims and approaches. This thesis intends to demonstrate how a combination of laboratory studies and field measurements, as well as the combined application of various comprehensive analytical techniques and evaluation methods can provide unique insights into the semi-volatile fraction of atmospheric aerosols. Thereby, the aim lies on connecting the results from an in-depth physicochemical characterization of both, primary and secondary organic aerosols to their respective toxicological outcomes. In greater detail, the main research questions, which are discussed in this thesis, are:

1) How complementary are different mass spectrometric techniques? What conclusions can be drawn and what aspects of the chemical complexity of aerosols and their associated processes can be elucidated from their application?

Although basic metrics such as number or mass concentration, size distribution, PM10 or PM2.5, or other metrics may serve specific purposes within aerosol science, a comprehensive, multifaceted characterization of aerosols is necessary to comprehend their complex effects across various different disciplines and areas of interest [1]. In order to characterize the full chemical complexity of the SOA and be able to link the results to environmental or toxicological outcomes, an analytical tool set is required, which is universally applicable to different aerosol types as well as a wide range of concentrations, and outputs semi-quantitative data for the entirety of the analytes. To meet this analytical challenge, this work is focused on the complementary application of mass spectrometric methods based on time-of-flight mass spectrometry (TOFMS) with electron ionization (EI), which are based on the thermal vaporization of aerosol particle constituents and cover online to offline approaches.

2) Does the chemical composition of laboratory-generated SOAs from an anthropogenic and a biogenic precursor depend on the chemical nature of the respective precursor?

This thesis includes a detailed chemical characterization of secondary organic aerosols, which were derived in the laboratory in an oxidation flow reactor (OFR) from a typical anthropogenic (naphthalene) and biogenic (β-pinene) precursor compound in the presence of combustion soot particles (SP). By means of thermal desorption - comprehensive two-dimensional gas chromatography - TOFMS and further techniques previously evaluated, the chemical identity of the two generated SOA types was characterized in regards to individual molecular composition, compound classes, and oxidation state.

3) Can the *in vitro* toxicological effects of laboratory-generated SOAs from an anthropogenic and a biogenic precursor be attributed to differences in their chemical signatures?

One major cross-disciplinary challenge involves investigating the mechanistic connections between the physicochemical characteristics of aerosols, and their toxicity and resulting biological effects. This work focuses on elucidating the chemical constituents of the generated aerosols, which drive adverse outcome effects in different *in vitro* model systems, including mono- and cocultures of lung epithelial and endothelial cell lines.

4) How does the integration of open-field burning experiments with laboratory combustion experiments contribute to elucidating the chemical composition of biomass burning organic aerosols (BBOA), and what are the implications for understanding their impact on air quality, climate, and the environment?

For the most comprehensive understanding of the effects of atmospheric aerosols, it is important to combine the three scientific approaches listed above (A-C), which are commonly used in aerosol science. Despite recognizing the significance of modeling studies for tasks such as reproducing and predicting results from laboratory and field measurements, extrapolating findings to a broader global scale [6], as well as working towards mass closure between gas and particle phase molecular compositions upon aerosol formation [10], the focus of this thesis lies on empirical research and therefore solely discusses the integration of laboratory and field studies. Moving on from laboratory-generated aerosols, which can be attributed to a single precursor (research questions 1-3), this thesis extends its scope to include a study with more realistic experimental conditions. Specifically, we examine BBOA emissions resulting from the combustion of sugar cane, in both controlled laboratory settings and real-world field conditions. We address challenges in linking laboratory with field experiments and compare the resulting chemical composition by employing targeted and non-targeted evaluation approaches.

4 Methods and Instrumentation

This chapter introduces the methods applied for aerosol sampling, aerosol chemical analysis and data evaluation.

4.1 Sampling of PM

Most PM measurement techniques fall into two categories: the first allows *in situ* measurement of aerosols in real time (online analysis), and the second is based on the collection of aerosol particles on a substrate, usually filters, for subsequent offline analysis [75]. For the latter, there are various filter materials available depending on the intended use and subsequent analytical technique. These materials include quartz and glass fibers, cellulose, polystyrene and polycarbonate [76]. Quartz fiber (QF) filters are frequently used to sample PM for subsequent chemical analyses, such as elemental and organic carbon (EC/OC) analysis or chromatographic techniques. This preference is due to their low levels of trace contamination, relative inertness, and ability to withstand high temperatures for the elimination of trace organic contaminants [77]. Their ability to be heated to higher temperatures also makes them a suitable choice for thermal desorption (TD) approaches. In this work, TD of organic analytes from QF filters was used as the main sample introduction technique for aerosol analysis. We further applied at cut-off of 2.5 µm by employing an impactor ahead of the QF filter. This effectively separated particles with aerodynamic diameters exceeding 2.5 µm, depositing them onto an impaction plate.

It should be noted, however, that the sampling of OA using filters is complicated through sampling artifacts. A positive sampling artifact is the adsorption of organic vapors on the filter. A negative sampling artifact is the volatilization and therefore removal of analytes from the filter. [78] Additionally, compared to online methods, the storage and handling of filters is crucial in ensuring consistent and reproducible results, as it could affect the partitioning of the gas and particle phases [79]. Moreover, particle-bound reactive oxygen species (ROS), which are rapidly degraded, have been found to be greatly underestimated by offline techniques, where there is typically a delay between filter collection and analysis [80]. Finally, it is important to note that sampling errors can also occur during the transport of particles through the sampling tubes. For particles > 1 µm, the main mechanisms leading to particle deposition onto the tubing walls are gravitational settling and impaction induced by turbulence [81].

4.2 Mass Spectrometry of Organic Aerosols

The core principle of mass spectrometry (MS) involves the ionization of molecules and their characterization as ions by mass and charge ratios (m/z). The essential setup of a mass spectrometer includes a sample inlet, ion source, mass separation unit and detector [82].

Within this work, we used different MS techniques, all of which have in common that they apply electron ionization (EI) as the ionization method and detection by time-of-flight (TOF) MS. For this reason, EI-TOFMS is discussed in more detail in the following chapter.

4.2.1 Principles of Electron Ionization (EI) Time-of-Flight Mass Spectrometry (TOFMS)

Electron Ionization (EI)

EI is one of the most widely used ionization technique for mass spectrometric analysis of environmental samples. A schematic representation of an EI source is provided in **Figure 6 A**. After the sample has been vaporized, it is introduced into the EI ion source, which is in a high vacuum (10^{-7}–10^{-5} mbar). High-energy electrons from a heated filament are accelerated and focused into an electron beam, which then collides with the vaporized molecules, producing positively charged ions if the collision energy exceeds their ionization energy. By applying an extraction voltage (~ 500–10,000 V), these ions are subsequently accelerated from the source to the mass analyzer [83]. The ionization process can be described using the following equation [84].

$$M + e^- \rightarrow M^+ + 2e^- \quad (1)$$

A standardized ionization energy of 70 eV is commonly used to measure EI spectra. Although each molecular species has its own ionization efficiency curve depending on its specific ionization cross section, the ionization efficiency curve of most molecules has a maximum at ~70 eV. Since basically all atoms and molecules can be ionized at 70 eV and small variations in electron energy around 70 eV (60–80 eV) are neglectable, resulting in a well reproducible mass spectra, EI spectra are typically measured at 70 eV. [84]

As a result of the reproducible fragmentation seen in EI–MS, it is possible to identify organic compounds using spectral libraries (e.g., the US National Institute of Standards and Technology (NIST) library), which are widely available for EI–MS spectra. This is particularly useful for GC–MS analysis. However, compared to “soft” ionization methods like chemical ionization (CI), photoionization (PI), and electrospray ionization (ESI), which result in less fragmentation, EI is a so-called “hard” ionization technique. As such, EI–MS often fails to detect the molecular ion due to induced fragmentation, making data interpretation more difficult for superimposed spectra or compound spectra not found in spectral libraries [85]. However, the consistent and fragment-rich mass spectra have led to well-established fragmentation pathways and interpretation rules for EI mass spectra [86].

Time-of-Flight Mass Spectrometry (TOFMS)

After ionization, ions of various m/z ratios are focused, accelerated and subsequently dispersed in time as they travel along a field-free drift path of known length. If all the ions start on their path through the flight tube at the same time or within a relatively short time span, the lighter ions will reach the detector before the heavier ones. Defining this starting point requires the use of a pulsed ion source [87]. The ions are accelerated within a predetermined electric field and introduced to the flight tube.

In state-of-the-art TOF mass spectrometers, a reflectron is often used to improve mass resolution [88] compared to instruments with linear flight paths. A schematic diagram of a reflector TOFMS is shown in **Figure 6 B**.

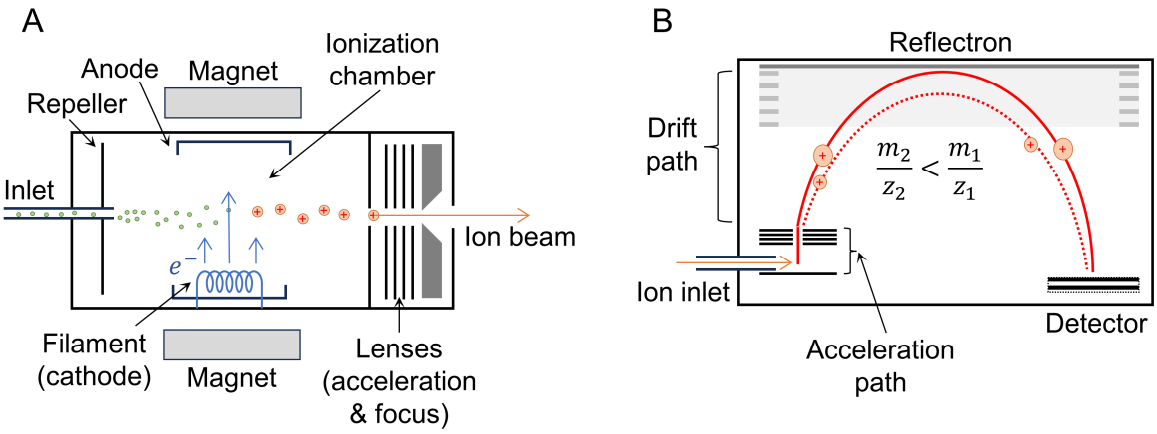

***Figure 6: A**) Schematic representation of an electron ionization (EI) source. Small magnets focus the electron beam, which is extracted from a heated filament (cathode). The repeller directs all produced ions (positive charge) towards the acceleration and focus region of the ion source. **B**) Schematic representation and principle of a reflector time-of-flight mass spectrometer (TOFMS). Ions released from the ion source are accelerated by an electrical field and penetrate the reflector at different depths before reversing their direction of flight. Depending on their kinetic energy, the ions thus cover different distances, which is accompanied by a time focus. The separation of ions takes place according to their m/z ratio.*

The working principle involves the acceleration of ions by an electric field, resulting in ions of different kinetic energy depending on their m/z. After acceleration, the ions pass through the drift tube, at the opposite end of which a reflectron is located, which consists of a series of electrodes that generate a gradient electrical field. This field effectively decelerates the ions, causing a reversal in their flight direction. Consequently, the ions experience an increased effective drift length. Ions with higher kinetic energies enter the reflectron at greater depths and take longer to decelerate than ions with lower energies. As a result, ions of similar m/z converge on the detector at approximately the same time, regardless of their initial kinetic energies. This together with the increased drift path leads to an improved mass resolution. The use of multi-reflectron TOFMS instruments further extends the flight path of the ions, resulting in improved separation of ions with different m/z and further increasing the mass resolving power of a TOFMS [89].

The appeal of TOFMS for aerosol chemical characterization lies in its ability to combine fast data acquisition (acquisition rates up to 500 Hz) with mass spectral information over a wide mass range. Hence, TOFMS is suitable for coupling with fast analytical approaches [90, 91] (e.g., chromatographic methods), as well as for the online monitoring of dynamic processes characterized by high temporal variability (e.g., formation and atmospheric processing of aerosols).

4.2.2 From Online to Offline Mass Spectrometry Techniques

The scope of this thesis includes an investigation of different EI–TOFMS techniques applied to the chemical characterization of organic aerosols, which, although generally based on the ionization of molecules by EI and their characterization as ions by mass and charge in a TOF mass spectrometer, they differ in their informative value and areas of application. As the three techniques considered are discussed in detail in **section 5.1.2**, they are only briefly presented here. Further details are provided in Hartner *et al.* [79].

HR–TOF–AMS (online)

The high-resolution time-of-flight aerosol mass spectrometer (HR–TOF–AMS) is the most used MS system for online *in-situ* aerosol analyses in real time. It allows for the identification of the elemental composition and oxidation states of OA [67, 92]. However, the availability of molecular information is constrained due to the fragmentation caused by pyrolysis and ionization procedures [66].

The major components of the HR–TOF–AMS are an aerodynamic lens inlet and differential pumping system where particle sizing is performed (modulated by a mechanical chopper at the entrance of the sizing chamber), an ion source region where particle flash-vaporization (600 °C) and EI (70 eV) occurs, and a TOF mass analyzer [93]. The HR–TOF–AMS can either be operated in the particle time-of-flight mode (PTOF-mode) or in the mass spectrum mode (MS-mode). The former is used to calculate the particles' aerodynamic diameter for the size-segregated analysis of the particle composition. The latter provides mass spectral information of the total aerosol mass [67, 94].

In this work, the AMS was applied in V-mode, which corresponds the reflector TOF described previously, resulting in a mass resolution of 2.1×10^3 (specification for m/z 200) [67]. We further operated the AMS in PTOF-mode alternating with MS-mode, with a time resolution of 4 min per measurement cycle.

DIP–HRTOFMS (atline)

Direct inlet probe high-resolution time-of-flight mass spectrometry (DIP–HRTOFMS) is classically used in petroleum analysis [64, 95], but is not a typical technique applied for the analysis of environmental samples. We show its application as an atline method with short measurement times for the analysis of PM collected on QF filters. In DIP–HRTOFMS, the sample undergoes thermal vaporization (400 °C) directly in the ion source (EI, 70 eV) of a multi-reflectron mass spectrometer, which is valuable for determining the elemental composition of overlapping mass fragments with identical unit masses due to the high-resolution accurate mass spectral data obtained. In the field of aerosol chemistry, particularly when investigating the chemical composition of oxidized and nitrated SOA, the differentiation of isobaric species is of interest. In this regard, the mass splits of CH_4/O (0.0364 Da) and CH_2/N (0.0126 Da) [90] are easily resolved by HRTOFMS.

In this work, the thermal vaporization gradient in the ion source was set to 2 K sec^{-1} up to a temperature of 400 °C. The multi-reflectron mass spectrometer was operated in the 32 reflection mode, resulting in a high mass resolution of >2.5×10^4 and a mass accuracy of <2 ppm (instrumental specification for m/z 219).

TD–GC×GC–TOFMS (offline)

The main technique applied in this thesis was thermal desorption comprehensive two-dimensional gas chromatography time-of-flight mass spectrometry (TD–GC×GC–TOFMS).

A thermal desorption (TD) method was used to achieve thermal volatilization of semi-volatile analytes from a filter punch placed directly inside the liner in the GC injector. Unlike more conventional sample introduction techniques such as solvent extraction, TD does not require complex sample preparation, but gradually vaporizes the analytes by applying a gradient temperature ramp in a protective He atmosphere.

GC hyphenated with TOFMS is the state-of-the-art technique for the offline chemical characterization of sampled aerosols, allowing the separation and identification of (S)VOCs. However, for the analysis of highly complex sample matrices, such as organic aerosols, the limited peak capacity of one-dimensional GC to separate the multitude of diverse compounds reaches its limits. Comprehensive two-dimensional gas chromatography (GC×GC) offers greatly improved resolution capabilities and a high peak capacity compared to one-dimensional GC, making it a valuable technique for analyzing organic aerosols considering the prevalence of a large number of compounds at low concentrations.

GC×GC involves two capillary columns with different physicochemical characteristics, which are coupled by a modulator. The modulator fractions and reintroduces the effluent from the primary GC column into the secondary GC column. By selecting stationary phases of varying polarity to achieve two independent orthogonal separation mechanisms, compounds co-eluting from the first GC column are subjected to a different separation mechanism in the second GC column and are chromatographically separated (**Figure 7**). Conventionally, a non-polar column is used in the first dimension and a polar column in the second dimension, resulting in a separation of the analytes based on their volatility in the first dimension and based on their polarity in the second dimension. Furthermore, this improved peak resolution is a significant advantage for EI–TOFMS library searches, resulting in increased confidence in peak identification.

In this work, the TD temperature gradient was set to 2 K sec^{-1} up to a temperature of 300 °C. We applied a 60 m non-polar column in the first dimension and a 1.5 m mid-polar column in the second dimension. Ionization and detection were carried out by EI (70 eV) and with a reflector TOFMS, achieving a mass resolution of 1.3×10^3 (specification for m/z 219).

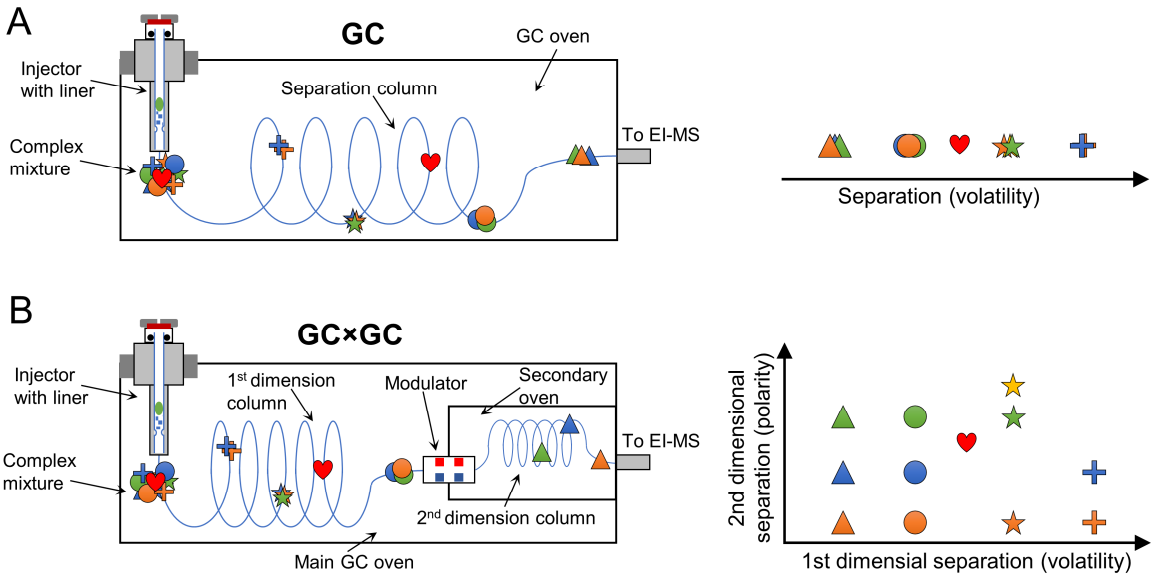

Figure 7: *Chromatographic separation of complex sample mixtures for* ***A)*** *one-dimensional GC and* ***B)*** *GC×GC. The application of two orthogonal separation mechanisms (here depicted as color and shape), prevents the co-elution of compounds from the first dimension, resulting in their separation in the secondary dimension.*

4.3 Data Handling for GC×GC-TOFMS

GC×GC–TOFMS measurements generate huge data sets. The derived output matrix is comprised of a series of m/z and intensity pairs for each chromatographic data point. After the chromatographic separation of compounds in two dimensions, they are assigned to peaks. The data is usually presented in the form of a peak table and a visual representation of the 2D chromatogram called a contour plot.

4.3.1 Peak-based and Pixel-based Evaluation Approaches

To enable comparative analysis between different measurements or sample classes, the large number of chemical features (up to several thousand) first needs to be aligned. Pre-processing procedures include data normalization and scaling, as well as removal of redundant areas in the contour plot (e.g. solvent peaks, column bleed). For the subsequent peak alignment, (statistical) evaluation and interpretation of the data, there is no standardized data processing workflow. However, there are two main approaches to GC×GC–TOFMS data evaluation, the peak-based and the pixel-based approach, which are illustrated in **Figure 8**.

4.3.2 Targeted and Non-targeted Analysis

Moreover, for the analysis of GC×GC–TOFMS data, a common distinction lies between two different types of data handling techniques: targeted and non-targeted analysis. It is worth noting that both peak-based and pixel-based approaches can be employed for both targeted and non-targeted analysis.

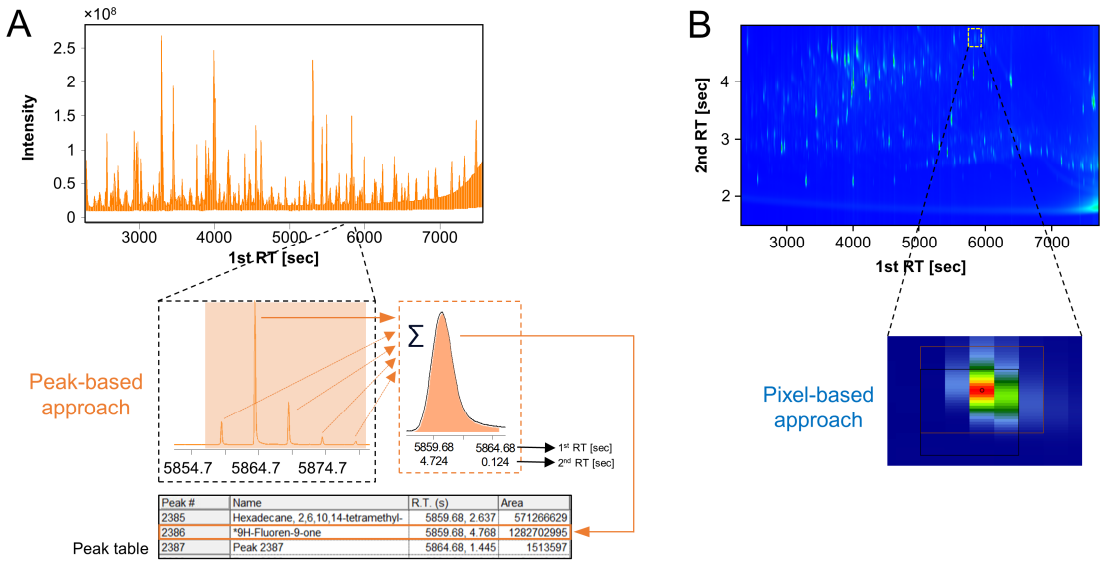

Figure 8: *Different data evaluation approaches for GC×GC–TOFMS data.* ***A)*** *Peak-based approach, which is the more conventional approach and involves peak deconvolution and integration of peak areas. The peak areas of individual sub-peaks are summed up to give an area value for each chemical compound.* ***B)*** *Pixel-based approach, which uses raw data to provide quantitative information within individual data points (pixels). Chromatographic windows (tiles) are defined so that the same compound in all the samples appears in the same window in order to compare different sample classes. The tile boundaries (black box) are defined by the user and set the chromatographic window, in which the point of maximum difference between the classes is found (black circle marker). The integration window (brown box) is centered around the point of maximum difference between the classes.*

Targeted analysis is commonly used to investigate a pre-defined list of compounds with known characteristics in a sample matrix. Conversely, non-targeted analysis involves the evaluation of all detectable compounds present in the sample or in sample classes with initially unknown compounds of interest [96]. A major challenge is the elucidation of the important information from the large amount of data generated by non-targeted analysis. Generally, non-targeted analysis aims to uncover compositional differences within a given sample set and finds its application in the classification and identification of (marker) compounds, monitoring and chemical fingerprinting of complex sample matrices [97]. Hence, non-targeted data evaluation approaches offer a comprehensive examination of the entire chemical signatures derived by GC×GC–TOFMS. In particular, in the context of environmental matrices such as atmospheric aerosol samples, non-targeted data analysis gains significant importance and is most useful for studying the effect of atmospheric processing, source apportionment, and identifying distinctive marker substances associated with specific sources or formation pathways.

In this work, we used both targeted and non-targeted approaches for the data evaluation of GC×GC–TOFMS data. The accompanying instrument software (*LECO ChromaTOF BT4D*) was used for data pre-processing and peak-based evaluation approaches. For non-targeted evaluation, the *LECO ChromaTOF Tile* software was used, which uses a pixel-based approach to compare raw data from several groups of samples.

5 Results and Discussion

5.1 Simulation of Atmospheric Processes in the Laboratory

Within the framework of the *aeroHEALTH* research project, we conducted laboratory studies of an anthropogenic and biogenic VOC to simulate atmospheric aging processes by means of an OFR under varying time scales and concentration ranges. Moreover, advanced exposure systems for biological models were employed to examine the health effects of aerosols and how they are influenced by atmospheric chemistry. The overarching objective was to connect chemical composition, photochemical oxidation and health effects within an interdisciplinary laboratory setup. To attain this objective, a central aspect of this thesis revolves around the molecular analysis of aerosols through the application of comprehensive analytical methods.

5.1.1 Laboratory-generated SOA from Anthropogenic and Biogenic Precursors

Experimental Setup

A simplified overview of the experimental system is given in **Figure 9**. More detailed descriptions of the experimental setup during the first campaign of the *aeroHEALTH* project can be found in related publications [23, 61, 79, 80]. In short, SOAs were generated through OH-dominated photochemical aging of either naphthalene (NAP) or β-pinene (βPIN) vapors, which were mixed with flame-generated propane soot particles (SP) from a miniature combustion aerosol standard (mini-CAST) generator. A PAM [58, 59] OFR was used to perform photochemical aging. Different atmospheric aging conditions were achieved by regulating the intensity of the UV-lamps and relative humidity in the PAM OFR.

In this laboratory simulation of two different aerosol model systems, the generated SPs served as condensation nuclei for SOAs and represented air pollution by primary combustion emissions. The atmospheric processing in the PAM OFR of a typical anthropogenic (NAP) or biogenic (βPIN) VOC precursor resulted in SPs coated with condensed organic matter from the respective precursor compound. In the following, the produced anthropogenic and biogenic SOA proxy are referred to as SOA_{NAP}-SP and $SOA_{\beta PIN}$-SP, respectively. Slight deviations in concentrations and experiment durations were applied to the setup depending upon its application for either physical/chemical investigations on photochemical aging (see **section 5.1.2**), or experiments involving biological cell exposures (see **section 5.1.3**). For the former, for each 1 h experiment of constant conditions, 0.25 mg m^{-3} SPs and 1 mg m^{-3} VOC (NAP or βPIN) were introduced into the PAM. For the latter, for the duration of a 4 h cell exposure at the air-liquid interface (ALI), constant conditions of 1 mg m^{-3} SPs and 4 mg m^{-3} VOC (NAP or βPIN) were maintained. These higher concentrations during biological experiments were chosen according to the dose threshold for acute toxicity.

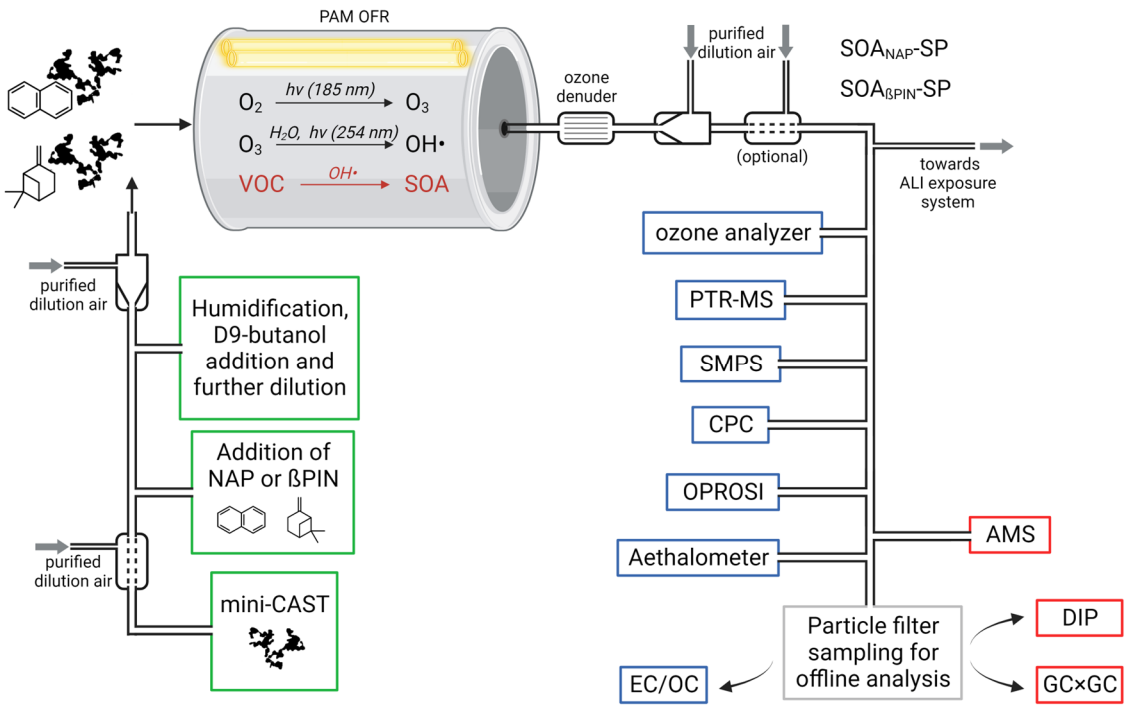

Figure 9: *Simplified schematic of the experimental setup for the generation (green boxes) and comprehensive characterization of the gas phase and particle phase (blue boxes) of the SOA. Chemical characterization by AMS, DIP and GC×GC (red boxes) are discussed in detail in the subsequent sections. Definitions of the acronyms are provided in the text and in the list of abbreviations. Created with BioRender.com.*

The online instrumentation for in-depth characterization of the produced aerosols, amongst others, included a quadrupole proton-transfer-reaction mass spectrometer (PTR-MS) to monitor the decay of D9-butanol and determine equivalent photochemical aging times [98], a scanning mobility particle sizer (SMPS) and condensation particle counter (CPC) to monitor particle number and size distribution, an aethalometer, as well as a particle-bound reactive oxygen species (ROS) instrument (OPROSI) [80, 99, 100]. Online analysis by AMS will be covered in detail in the subsequent section (see **section 5.1.2**). In parallel, particulate matter was sampled on QF filters for the subsequent offline characterization by a thermal optical carbon analyzer for the determination of the elemental carbon (EC) and organic carbon (OC) content. The same filter material was used for offline analysis by GC×GC and atline analysis by DIP, which will later be discussed along with the AMS (see **section 5.1.2**).

General Physicochemical Characterization of SOA_{NAP}-SP and $SOA_{\beta PIN}$-SP

An overview of the physicochemical characteristics of SOA_{NAP}-SP and $SOA_{\beta PIN}$-SP is depicted in **Table 1**. Transmission electron microscopy (TEM) images of both model aerosol types (at an atmospheric OH aging equivalent time of ~ 3 days) revealed the typical chain-like structure of the fractal patterns of soot agglomerates, though upon addition of VOCs (NAP or βPIN) its fractal structure collapsed resulting in a coating of organic material. SOA_{NAP}-SP and $SOA_{\beta PIN}$-SP exhibited similar physical properties such as particle number and mass concentration, as well as particle diameter. Furthermore, total OC and EC concentrations, as well as concentrations of the different

OC fractions (OC1-OC4) were comparable. However, a higher hydrogen peroxide (H_2O_2) equivalent was found for SOA_{NAP}-SP, indicating an increased prevalence of ROS and a higher oxidative potential in regard to $SOA_{\beta PIN}$-SP. This is in line with oxygen-to-carbon ratio (O/C) and hydrogen-to-carbon ratio (H/C) determined by AMS, which revealed a higher O/C and lower H/C for SOA_{NAP}-SP than for $SOA_{\beta PIN}$-SP and is in good agreement with a previous study [101] about the photochemical aging of NAP and α-pinene. Consequently, the average carbon oxidation state (OS_C) of SOA_{NAP}-SP, which can be calculated from the H/C and O/C ratios ($2 \times O/C - H/C$), exceeded that of $SOA_{\beta PIN}$-SP. These results indicate a higher photochemical oxidation of SOA_{NAP}-SP compared to $SOA_{\beta PIN}$-SP under the same aging condition. Therefore, despite the similar physical characteristics of both aerosol types, an in-depth chemical characterization on the produced SOA constituents is necessary to advance our knowledge of the impact of these complex organic aerosol mixtures.

Table 1: *Physicochemical properties of SOA_{NAP}-SP and $SOA_{\beta PIN}$-SP derived from 1 mg m^{-3} SPs and 4 mg m^{-3} NAP or βPIN (OH aging equivalent ≈ 3 d), which represents the settings for aerosol generation applied during all biological exposure experiments. Data is published in [23]. Values are shown as mean ± standard deviation.*

		SOA_{NAP}-SP	**$SOA_{\beta PIN}$-SP**
TEM images		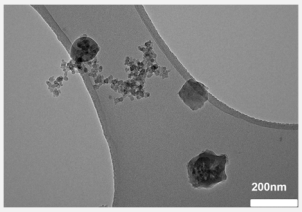	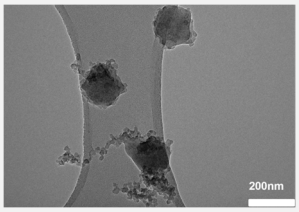
BC	[mg m^{-3}]	1.5 ± 0.1	1.4 ± 0.1
BrC	[%]	32 ± 1	22 ± 1
Atm. OH aging equivalent	[days]*	2.9 ± 0.4	2.8 ± 0.2
Particle number concentration	[*n* cm^{-3}]	$1.4\times10^6 \pm 0.2\times10^6$	$0.9\times10^6 \pm 0.2\times10^6$
Particle geometric mean diameter	[nm]	114 ± 0.7	117 ± 0.3
Total EC	[mg m^{-3}]	1.0 ± 0.2	0.7 ± 0.1
Total OC	[mg m^{-3}]	1.1 ± 0.2	1.0 ± 0.2
OC1		0.2 ± 0.05	0.1 ± 0.03
OC2		0.3 ± 0.05	0.3 ± 0.05
OC3		0.5 ± 0.1	0.5 ± 0.1
OC4		0.1 ± 0.05	0.1 ± 0.04
O/C	[ ]	0.77 ± 0.06	0.61 ± 0.02
H/C		1.04 ± 0.003	1.65 ± 0.02
OS_C		0.49 ± 0.12	–0.43 ± 0.04
H_2O_2 equivalent	[µmol m^{-3}]	14.1 ± 0.9	3.6 ± 0.5

*Assuming an average OH• concentration of 10^6 molecules m^{-3}

5.1.2 Complementary Application of EI–TOFMS Techniques for In-depth Physicochemical Aerosol Characterization

State-of-the-art analytical techniques such as MS play an important role in unraveling the great chemical complexity of SOA on a molecular scale. In this study, we accentuate the qualities and limitations of three different MS methods for the chemical characterization of SOA derived from laboratory photochemical aging of combustion soot particles, premixed with gaseous NAP or βPIN as SOA precursor. We conducted comprehensive chemical investigations through application of three different EI–TOFMS techniques, namely a) high-resolution time-of-flight aerosol mass spectrometry (HR–TOF–AMS), b) direct inlet probe high-resolution time-of-flight mass spectrometry (DIP–HRTOFMS) and c) thermal desorption comprehensive two-dimensional gas chromatography time-of-flight mass spectrometry (TD–GC×GC–TOFMS). As such, we focused on both established and emerging techniques, encompassing both online and offline methodologies, in the context of their informative potential for studying the oxidation state, volatility, and molecular composition of the particulate fraction of laboratory-generated SOA. Schematic diagrams and key parameters of HR–TOF–AMS, DIP–HRTOFMS and TD–GC×GC–TOFMS are depicted in **Table 2**. Continuing forward, these techniques, which all three can be classified in the field of thermal analyses (analytes are thermally vaporized) and use EI as ionization technique for MS detection of the particle phase, will be referred to by their abbreviations AMS, GC×GC, and DIP.

The AMS, first reported by DeCarlo *et al.* [67] is an online technique, which is well-established in the aerosol science community [102] for the real-time measurement of non-refractory aerosols in the size range between 50 and 1000 nm in diameter [66]. Thereby, the particles are sampled and focused by an aerodynamic lens system and guided to a 600 °C heated tungsten vaporizer [103]. The vaporized analytes are ionized by EI and subsequently detected by TOFMS, yielding a sum mass spectrum, which shows the linear superposition of the individual organic species' mass spectra according to their concentrations. Mainly, the AMS is employed for the determination of elemental ratios [68, 104], including the previously discussed O/C and H/C ratios (see **Table 1**), which serve as indicator of aerosol age and volatility. Additionally, the AMS is used for quantitative analysis of the overall chemical composition of organic aerosols. For this, it utilizes Gaussian fits of ion signals, which are background-corrected and subsequently integrated. Ions are attributed to the peak at a given unit mass guided by a user-selected list of potential ions for peak fitting [67, 105]. The AMS offers a mass resolution of around 2.1×10^3 (specification for m/z 200) [67], which governs the precision of the identified composition of the measured ions. Utilizing this established ion list, the mass spectrum is categorized into distinct organic families.

For DIP, unlike the real-time analysis offered by the AMS, particles need to be sampled on filters, which subsequently can be analyzed atline, benefiting from short analysis times of 10 min. During the analysis, which is described in detail in Käfer *et al.* [64], a small circular filter punch is directly introduced into the ion source, where a gradual heating ramp is applied up to a temperature of 400 °C at 10^{-6} to 10^{-3} mbar, which leads to the volatilization and ionization of the semi-volatile organic

constituents. Following EI, the resulting ions undergo separation and detection in a multi-reflectron TOF mass spectrometer with high mass resolution. In addition to the acquired summed mass spectra, temperature-resolved and thus volatility-resolved mass spectra can be gathered from DIP measurements as a result of the gradual volatilization of the sample constituents in the ion source, which enables information about the volatility of the analytes. In this context, it needs mentioning, that within the vacuum in the ion source, molecules undergo vaporization at significantly lower temperatures than their boiling points under atmospheric conditions, following the principles of the Clausius–Clapeyron relation. For this reason, DIP finds its primary application as a thermal analysis technique for samples with high boiling points, such as petroleum [64, 95]. In our study, however, we further introduced DIP as a novel emerging technique for the chemical characterization of complex aerosol matrices.

GC×GC operates as an offline method and, as for DIP, involves the vaporization of analytes from a circular filter punch within the GC injector. It enables a molecular-level interpretation of the findings through the separation and identification of individual compounds. To prevent excessive thermal stress for the analytes, the maximum temperature during TD is limited to 300 °C. Consequently, GC×GC is confined to analyzing semi-volatile compounds. After TD, the analytes are introduced onto a pair of capillary columns with varying physicochemical attributes, which are interconnected using a modulator. This results in the chromatographic separation of analytes via two independent orthogonal dimensions, with each analyte being assigned a corresponding peak. As a result, this leads to a significantly improved resolution and substantial increase in peak capacity in contrast to one-dimensional GC [106] or other thermal separation methods like DIP. Particularly when coupled with TOFMS, GC×GC proves highly valuable for scenarios where numerous compounds are typically present at low concentrations, as typically is the case for environmental samples. Moreover, employing a standardized ionization energy of 70 eV enables the tentative identification of compounds through a mass spectral library search, such as with the NIST library. In comparison to AMS and DIP, which produce sum mass spectra, GC×GC pre-separates compounds and deconvolves peaks to generate individual compound specific mass spectra within one analysis.

Table 2: *Overview of the instrument schematics and key parameters of HR–TOF–AMS, DIP–HRTOFMS and TD–GC×GC–TOFMS. Values marked with * are based on literature [67] and were not experimentally determined. Table and graphics adapted from [79].*

	HR–TOF–AMS	DIP–HRTOFMS	TD–GC×GC–TOFMS
Instrument schematics	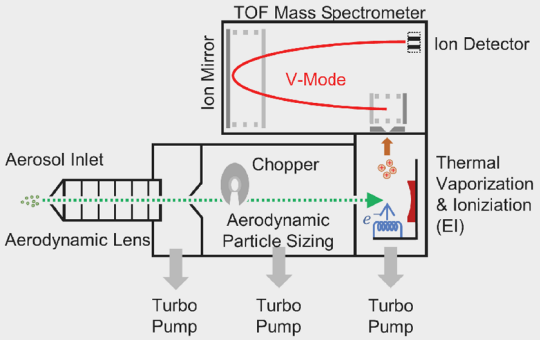	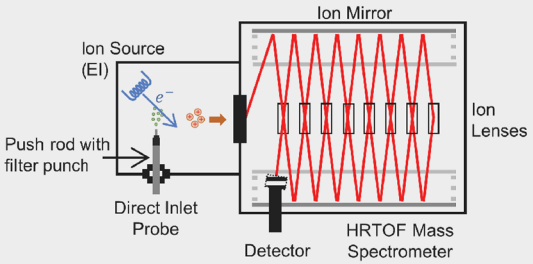	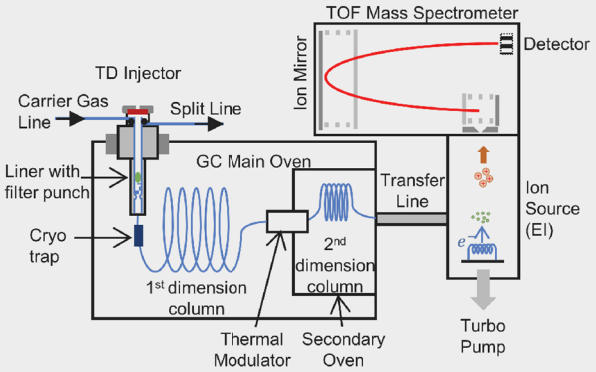
Analyses time	Online (4 min/cycle)	Atline (10 min)	Offline (3h)
Thermal sample introduction	- Flash vaporization/pyrolysis (600 °C) - Vacuum condition (10^{-9} – 10^{-6} mbar)	- Vaporization and pyrolysis by ramped heating - 40 °C – 400 °C (gradient 2 K s^{-1}); - Vacuum condition (10^{-6} – 10^{-3} mbar)	- Gradual thermal desorption - 40 °C – 300 °C (gradient 2 K s^{-1}) - > 1 bar overpressure in inert helium
Mass resolution, Mass accuracy and Mass range	- 2.1k* (m/z 200) - < 28 ppm* (m/z 100–200) - 9-459 Da (analyzed range 10–200 Da)	- 25k (m/z 218.99) - < 2 ppm (m/z 218.99) - 15–600 Da	- 1.3k (m/z 218.99) - 45 ppm (m/z 218.99) - 20–700 Da
Chemical / physical information	- Superimposed spectra - Fragment ion peaks (thermal & EI fragments) - Size segregation of PM	- Superimposed spectra - Fragment ion peaks (EI & thermal fragments) - Thermal pre-separation due to volatility	- Individual spectra for each compound; - Fragment ion peaks (mostly EI fragments) - Separation of individual compounds by GC

Comparing the summed mass spectra obtained from AMS, DIP and GC×GC analysis of a representative measurement of SOA_{NAP}-SP (**Figure 10 A-C**) revealed significant differences that originate from distinct variations in sample introduction and working principle prior to detection by EI– MS (ionization energy of 70 eV). The analysis of the summed mass spectra offers an understanding of whether the applied techniques are more susceptible to thermal or EI fragmentation. The AMS mass spectrum was shifted towards lower m/z values compared to the DIP and GC×GC spectra. It showed dominant peaks at m/z 44 (CO_2^+) and m/z 28 (CO^+), indicating extensive thermal fragmentation due to the applied flash vaporization at 600 °C. The DIP spectrum also displayed a high peak for CO_2^+, while the peak for CO^+ was lower than that in the AMS spectrum. In general, the DIP spectrum covered a wider range of mass fragments compared to the AMS spectrum, which predominantly contained small fragments due to the thermal decomposition of the compounds. The sum spectrum obtained from GC×GC does not provide information about the abundance of CO_2^+ and CO^+, as they were not detected due to the acquisition delay that was applied. Although some thermal fragmentation may occur in GC×GC, its spectrum is mainly dominated by EI fragments.

Representing GC×GC data as a sum mass spectrum, as we did here for comparison with AMS and DIP, is not the conventional way of presenting this data. This approach disregards essential chemical information acquired from employing chromatography hyphenated with mass spectrometry. The capability of the three techniques to extract molecular or structural information is illustrated by the example of m/z 132 (**Figure 10 D-F**).

Both AMS and DIP integrate mass spectral raw data and accumulate ions from different compounds within a single spectrum. The AMS spectrum displays a broad peak at m/z 132.04 (**Figure 10 D**), which is further divided into smaller peaks using an iterative algorithm based on their exact mass and a Gaussian distribution. These sub-fitted peaks are assigned molecular formulas, namely $C_8H_4O_2^+$ and $C_9H_8O^+$. These assigned formulas could be confirmed by DIP (**Figure 10 E**), whose spectrum at m/z 132 showed two well-resolved and distinctive peaks at the exact mass of 132.0205 ($C_8H_4O_2^+$) and 132.0569 ($C_9H_8O^+$). Due to the high mass resolution of the DIP platform, the O versus CH4 mass split of 36.4 mDa could unequivocally be resolved.

Although its mass resolution is lower when compared to AMS and DIP, the chromatographic separation of GC×GC enabled the resolution of various peaks at m/z 132. An extracted ion chromatogram (XIC) of m/z 132 (**Figure 10 F**) clearly illustrates this, demonstrating the successful separation of several single analytes with the molecular formula of either $C_9H_8O^+$ or $C_8H_4O_2^+$. Thereby, GC×GC separates multiple structural isomers of $C_9H_8O^+$ (yellow peaks), all sharing the same mass fragment of m/z 132. AMS and DIP, despite utilizing high resolution MS, were not able to access these individual chemical species. Furthermore, examining the specific mass spectra of the various compound peaks detected by GC×GC highlights the need to distinguish between fragment ions and molecular ions. The peaks corresponding to compounds with the sum formula $C_9H_8O^+$ display a molecular ion peak at m/z 132.04. Conversely, the peak at m/z 132.00 ($C_8H_4O_2^+$) represents

only a fragment of $C_9H_6O_3^+$ (1H-2-benzopyran-1,4(3H)-dione), with the molecular ion at m/z 162.02. This distinction, and as such, the identification of the chemical structure, is only feasible through the application of chromatography.

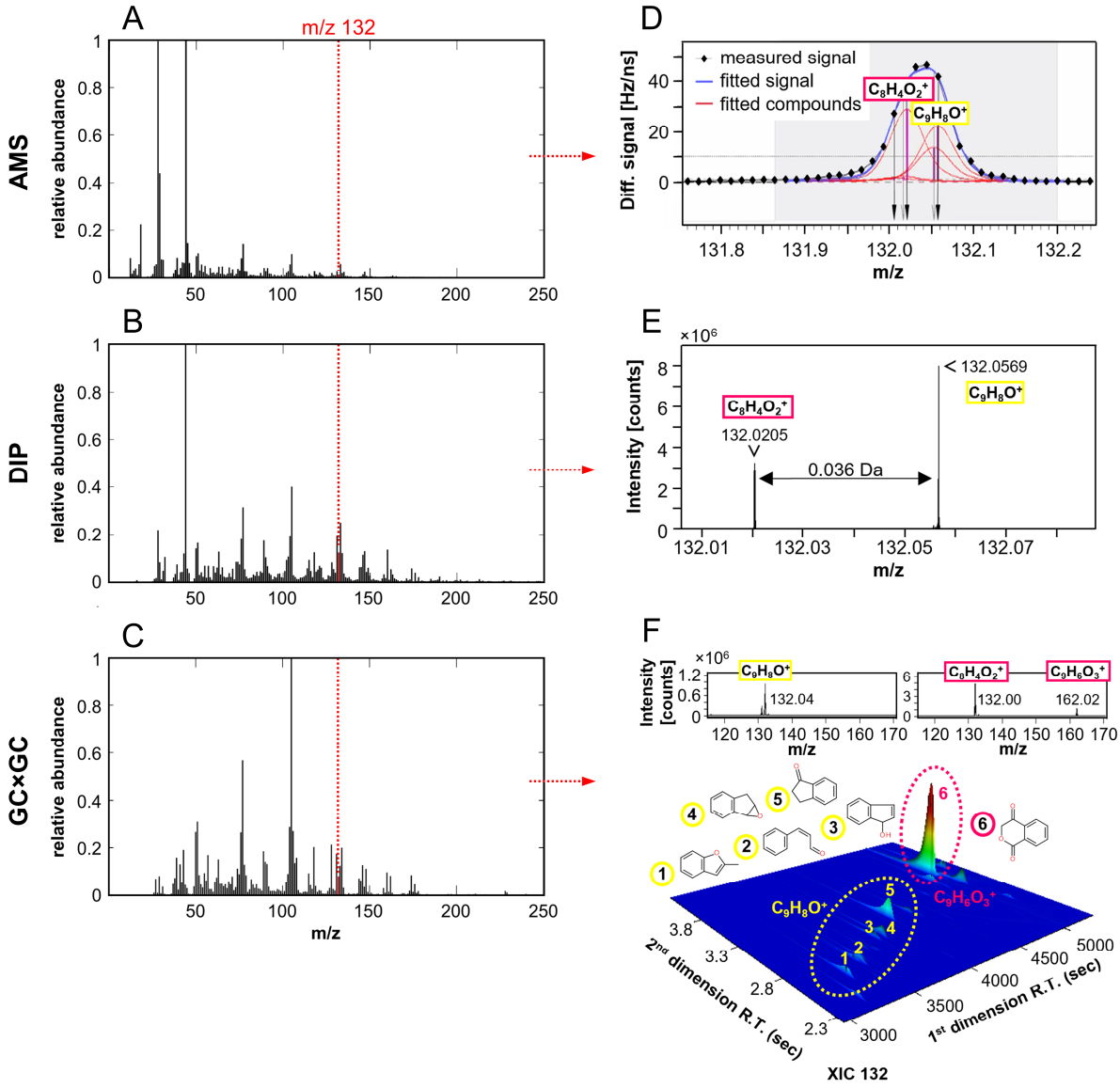

***Figure 10**: Summed mass spectrum of SOA_{NAP}-SP (atmospheric OH aging equivalent ≈ 4 d) derived from **A)** HR–TOF–AMS, **B)** DIP–HRTOFMS, and **C)** TD–GC×GC–TOFMS; Structural information can be obtained by AMS, DIP and GC×GC in different analytical depth as illustrated by the exemplary m/z 132: **D)** AMS "difference" spectra with sub-fitted peaks, which is calculated by subtracting the gas phase from the aerosol phase. The vertical arrows indicate different possible fitted compounds. **E)** DIP high-resolution mass spectrum; **F)** GC×GC extracted ion chromatogram (XIC) with assignment of peaks to molecular formula and deconvoluted mass spectrum (peak true). Adapted from results published in Hartner et al. [79].*

The three techniques provide structural information at different analytical depths. Molecular or structural characterization is particularly vital, for instance, in assessing the toxicity of aerosols or elucidating atmospheric reaction pathways. While the AMS produced reasonably good fits with an improved peak list, for a simplified and well-understood systems like the photooxidation of NAP in

a PAM OFR, and DIP ensured reliable elemental composition assignments for m/z up to 300 due to its high mass resolution, GC×GC was the most suitable technique for obtaining information on individual compounds. The application of GC×GC allowed for the comprehensive characterization of the molecular features, including their isomeric profiles.

A three-dimensional representation of AMS, DIP and (GC×)GC, as well as a thermal-optical carbon analyzer (EC/OC), is depicted in **Figure 11**. The comparison of the instruments (in terms of their application for the characterization of organic constituents in PM) is based on three characteristics: completeness (fraction of mass analyzed), chemical resolution and time resolution.

The complete characterization of OA (in terms of mass analyzed) is a great challenge due to the high number of individual species of different volatility ranges [4]. A thermal-optical carbon analyzer can measure and quantify the total OC content with a time resolution of approximately 1 h [4]. The temperature ranges applied during an EC/OC measurement for the different OC fractions (OC1: 140 °C; OC2: 280 °C; OC3: 480 °C; OC4: 580 °C) [108] can be roughly correlated with the vaporization conditions (temperature and pressure) during sample introduction for AMS, DIP and GC×GC. As such, GC×GC can access OC1–OC2, whereas DIP (with some limitations) and AMS include all four OC fractions. These limitations for DIP are connected to VOCs in the OC1 fraction and ELVOCs in the OC4 fraction. For OC1, the brief necessary time delay to acquire one mass spectrum after direct sample introduction to the ion source under vacuum conditions could lead to the discrimination of VOCs. For OC4, the full pyrolysis and capturing of ELVOCs cannot be completely assured despite the low pressure in the ion source.

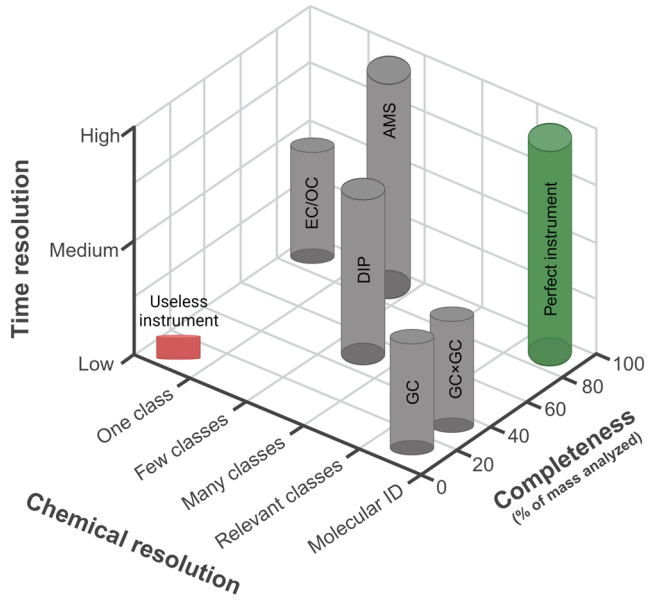

Figure 11: *Three-dimensional representation of techniques used for the analysis of the organic content of PM, namely AMS, DIP, (GC×)GC and thermal-optical carbon analyzer (EC/OC), highlighting their complementary nature. Definition of the acronyms is provided in the text and in the list of abbreviations. Adapted from [4, 107]. Created with BioRender.com.*

In terms of chemical and time resolution, it should be noted that although the AMS can quantitatively detect all four OC fractions in real-time, it is not capable to differentiate them due to the extensive thermal fragmentation caused by the flash-vaporization process. Therefore, the AMS only provides a certain level of chemical characterization without molecular information. GC×GC is the preferred option for obtaining detailed molecular or structural information on individual chemical species or functional groups present in OA. However, as an offline technique, GC×GC analyses are associated with a low time resolution (hours to days, depending on the experimental settings). In conclusion, it

is helpful to adopt a complementary approach of several analytical techniques in order to increase compound coverage across the chemical space.

5.1.3 Molecular Characterization of SOA by TD–GC×GC–TOFMS

In order to evaluate and compare the composition of the functionalized organic aerosol for both SOA_{NAP}-SP and $SOA_{\beta PIN}$-SP at the molecular level, we performed untargeted GC×GC analysis for the SVOCs in PM (**Figure 12 A**). The typical display of GC×GC data in a contour plot is shown in **Figure 12 B**. A contour plot is the two-dimensional representation of the GC×GC chromatogram, where the 1st dimension retention time (x-axis) corresponds to the volatility/carbon number of the compounds and the 2nd dimension retention time (y-axis) corresponds to the polarity of the compounds when a non-polar column is used in the first dimension and a polar column in the second dimension. The different appearance of the contour plots revealed completely different chemical signatures for SOA_{NAP}-SP and $SOA_{\beta PIN}$-SP. Thereby, SOA_{NAP}-SP consisted of fewer, but more abundant compounds in the accessible boiling point range. The process of assigning peaks to specific chemical compounds involves a comparison of relative intensities of corresponding m/z values in both the deconvoluted mass spectrum of the observed peaks (peak true) and the mass spectrum derived from the reference library (e.g. NIST). This is shown in **Figure 12 C** for the examples of naphthalene and nopinone. The advanced peak capacity and distinct peak separation capabilities of GC×GC contributed to achieving high quality library matches, typically with high similarity and probability scores. Nonetheless, for the identification of (stereo)isomers, reliance on the mass spectrum alone may be insufficient, so retention indices (RI) were used as an additional validation step to confirm identified matches from the library.

Subsequently, the 100 compounds with the highest signal intensities in SOA_{NAP}-SP and $SOA_{\beta PIN}$-SP were classified into aromatic (ring-opening and ring-retaining), cyclic and non-cyclic compounds, as shown in **Figure 12 D** in a representation of the contour plot with the peaks shown as bubbles with sizes corresponding to their respective peak areas. In the case of $SOA_{\beta PIN}$-SP, the predominant compounds consisted largely of oxygenated cyclic and acyclic structures. Conversely, within the composition of SOA_{NAP}-SP aromatic structures were the prevailing feature. Examples of the detected completely different chemical species in terms of molecular structures from both aerosol types are shown in **Figure 12 E**. A more detailed classification of these identified compounds, encompassing additional chemical subclasses and diverse functional groups, is illustrated in **Figure 12 F**.

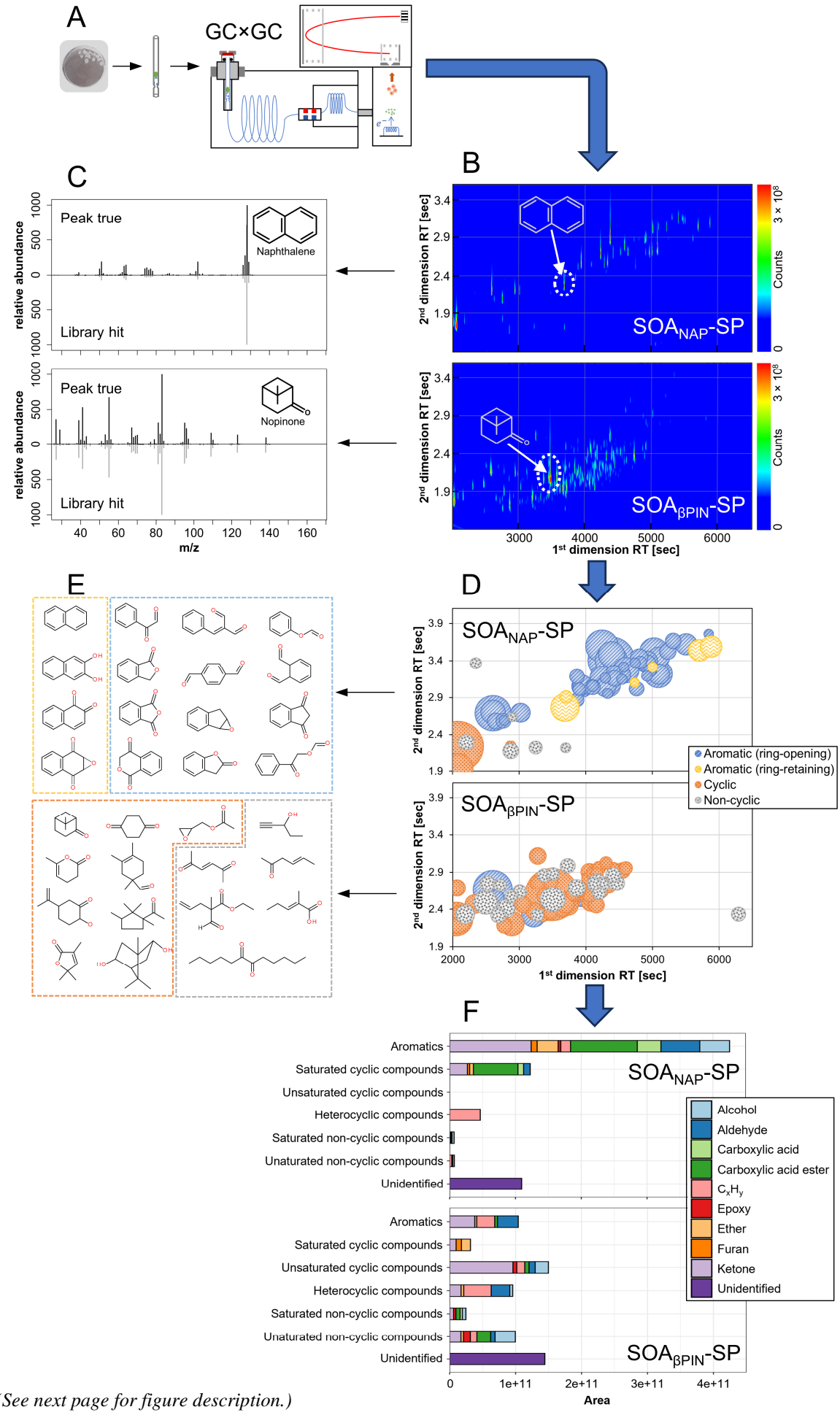

(See next page for figure description.)

Figure 12: *Chemical characterization of SOA_{NAP}-SP and $SOA_{\beta PIN}$-SP by TD-GC×GC-TOFMS (atmospheric OH aging equivalent ≈ 3 d).* ***(A)*** *Chemical approach for analysis of filter samples.* ***B)*** *GC×GC contour plot for SOA_{NAP}-SP (upper plot) and $SOA_{\beta PIN}$-SP (lower plot).* ***C)*** *Tentative assignment of peaks to their molecular structure based on comparison with NIST mass spectral library (match quality ≥ 70%) and retention indices. Deconvoluted spectrum (peak true) and NIST library hit spectrum is shown for naphthalene (upper plot) and nopinone (lower plot).* ***D)*** *Bubble plot representation of the 2D chromatogram for the 100 compounds with the highest signal intensities. The bubble sizes correspond to the respective peak areas for SOA_{NAP}-SP (upper plot) and $SOA_{\beta PIN}$-SP (lower plot). These 100 compounds account for 77.4% and 60.4% of the total abundance for SOA_{NAP}-SP and $SOA_{\beta PIN}$-SP, respectively.* ***E)*** *Structures of exemplary and representative peaks for SOA_{NAP}-SP (upper plot) and $SOA_{\beta PIN}$-SP (lower plot).* ***F)*** *Bar chart illustrating the areas of the 100 peaks with the highest signal intensities, which are classified by compound classes and functional groups for SOA_{NAP}-SP (upper plot) and $SOA_{\beta PIN}$-SP (lower plot). Figure was adapted from [23, 79].*

The found chemical structures are initial degradation products derived from the photooxidation of NAP and βPIN and are highly dependent on the chemical functionality of the precursor. The photochemical reaction of NAP is initiated by the addition of an OH radical, which leads to the formation of a pre-reactive molecular complex (hydroxyhexadienyl-type radical) [109], from which key ring-retaining products such as naphthols and naphthoquinones are formed [110]. However, according to Sasaki *et al.* [111] ring-retaining products represent only ~ 30% of the reaction products from the photooxidation process of NAP. As such, 2-formylcinnamaldehyde has been reported as the major ring opening product from the oxidation of NAP with OH [110]. For $SOA_{\beta PIN}$-SP, the most abundant compound detected by GC×GC was the major first-generation degradation product from the photooxidation of βPIN, nopinone, which in turn may react to form nine-carbon multifunctional compounds [112]. Proposed reaction mechanisms for NAP and βPIN photooxidation are depicted in **Figure 13**.

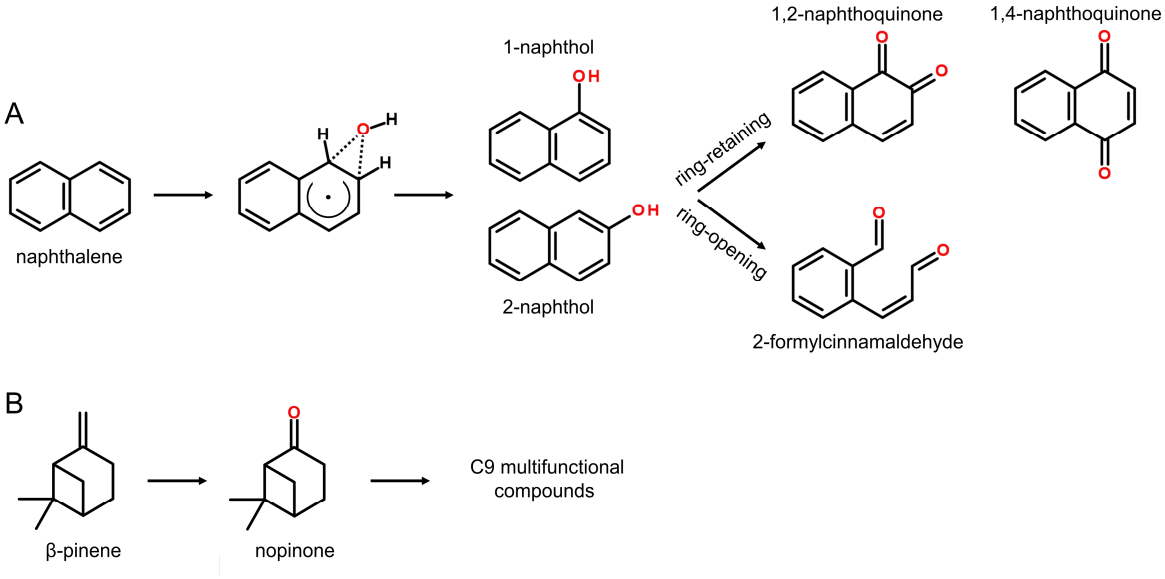

Figure 13: ***A)*** *Reaction pathway for the formation of ring-retaining oxidation products (naphthol and naphthoquinone isomers) as well as ring-opening oxidation products (2-formylcinnamaldehyd) from the photooxidation of naphthalene with OH. Adapted from [109, 110].* ***B)*** *Reaction pathway for the formation of nopinone and nine-carbon multifunctional products from the photooxidation of β-pinene. Adapted from [112].*

Given that the health risks of specific chemical characteristics (e.g. specific functional groups, aromaticity) may play a key role in the biological response of the produced SOAs (which have similar physical properties), the results obtained from TD–GC×GC–TOFMS may be very helpful in liking the chemical nature of SOA_{NAP}-SP and $SOA_{\beta PIN}$-SP with their respective biological responses (see **section 5.1.4**).

5.1.4 Connecting Physicochemical Composition of Aerosols to their Related Health Effects

An advanced *in vitro* cell model system was developed to investigate the toxicity induced by SOA_{NAP}-SP and $SOA_{\beta PIN}$-SP, consisting of a co-culture model comprising both epithelial cells (A549) and endothelial cells (EA.hy926). Cells were exposure at the Air-Liquid-Interface (ALI) for 4 h, allowing for exposures at more physiologic realistic conditions [113]. In contrast to monoculture systems, the established co-culture model allowed the study of cell-cell interactions between epithelial and endothelial cells, mimicking the physiological conditions of the blood-gas barrier, after exposure to both aerosol types. This helps to investigate local, as well as systemic effects, which are known to contribute to pulmonary and cardiovascular diseases [114].

We show results from the investigation of the aerosol-induced membrane integrity as a measure of cell viability (cytotoxicity) (**Figure 14 A, B**), oxidative stress (**Figure 14 C, D**) and primary and secondary genotoxicity (**Figure 14 E, F**) from ALI exposures with different dilutions of SOA_{NAP}-SP and $SOA_{\beta PIN}$-SP. These findings imply that even at high dilutions (low exposure levels), both aerosol types exhibit toxicity. Overall, the effects induced by SOA_{NAP}-SP were stronger than those induced by $SOA_{\beta PIN}$-SP. A clear dose-dependent increase in the oxidative stress marker malondialdehyde (MDA) was observed in the cell culture media of the co-culture cell model (A549 and EA.hy926 cells) for both aerosol types. In particular, the SOA_{NAP}-SP exposures led to higher levels of MDA. This is consistent with the higher H_2O_2 equivalents and increased OS_C values we found in SOA_{NAP}-SP compared to $SOA_{\beta PIN}$-SP. Notably, the generation of ROS has been previously linked to the abundance of particle-bound peroxides [115] and specifically to redox-active quinones [116]. This is in line with our findings, as indicated by the presence of 1,2- and 1,4-naphthoquinone in the particle phase of SOA_{NAP}-SP, which were detected by TD–GC×GC–TOF-MS as major products of the photochemical degradation of NAP (see **section 5.1.3**). While cells have a certain tolerance to oxidative stress, excessive stress may compromise membrane integrity (**Figure 14 B**) and induce genotoxic effects (**Figure 14 F**). The latter was observed following SOA_{NAP}-SP exposures with undiluted and 1:3 diluted aerosols, as reflected by the induced DNA damage (single- and double strand breaks), detected not only in epithelial cells, but also in the indirectly exposed endothelial cells, which suggests secondary genotoxicity.

In summary, the observed differences in overall toxicological effects could be attributed to the structural differences between SOA_{NAP}-SP and $SOA_{\beta PIN}$-SP. In this context, the detected prevalence of aromatic compounds, the higher OS_C and the increased presence of ROS in SOA_{NAP}-SP were

proposed to be highly relevant for its more pronounced toxicological effects compared to $SOA_{\beta PIN}$-SP.

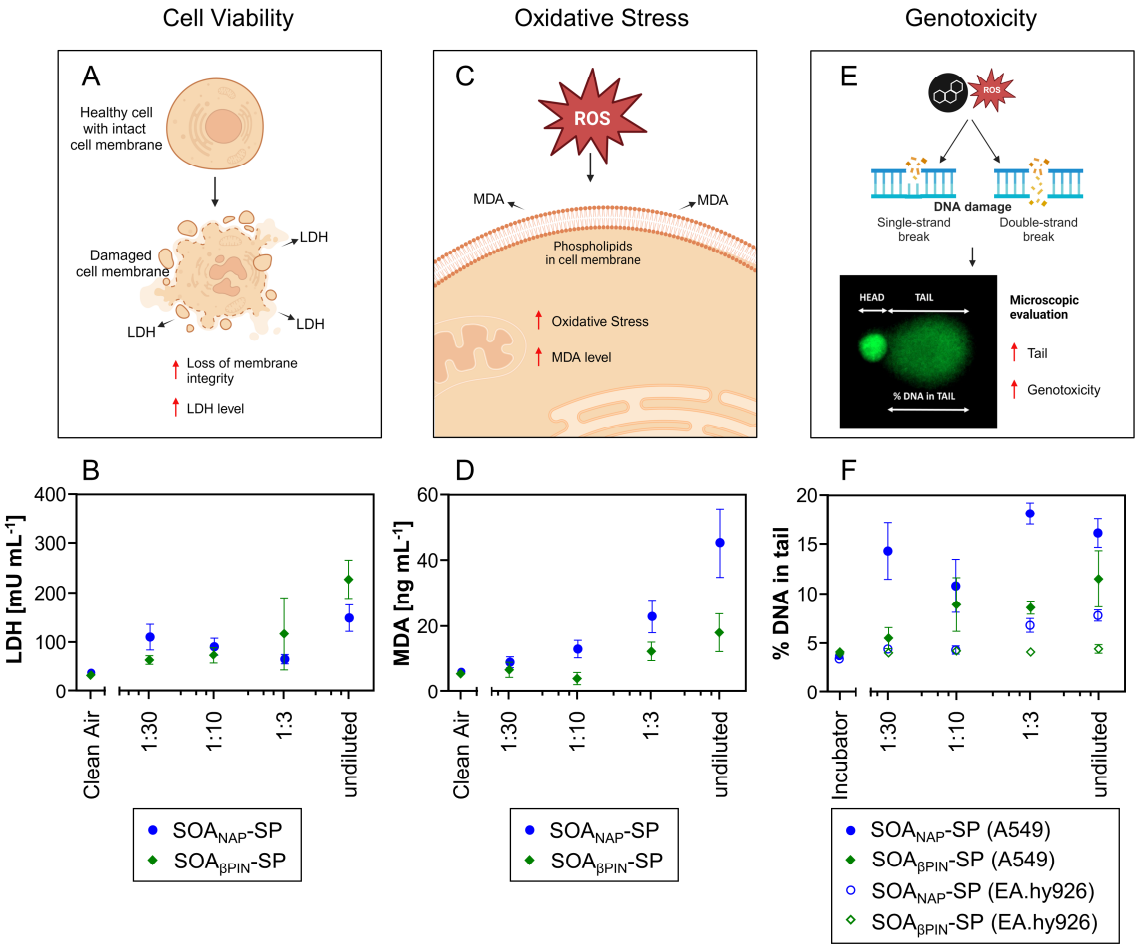

Figure 14: *Toxicological assessment of $SOA_{\beta PIN}$-SP and SOA_{NAP}-SP on a co-culture cell model containing epithelial cells (A549) and endothelial cells (EA.hy926).* ***A)*** *The lactate dehydrogenase (LDH) assay was performed on cell culture media collected after 4h aerosol exposure at the ALI to determine the amount of LDH released into the cell culture media, which indicates cell membrane damage [117, 118].* ***B)*** *The release of LDH was increased to a similar extent in both $SOA_{\beta PIN}$-SP and SOA_{NAP}-SP across different dilutions.* ***C)*** *Malondialdehyde (MDA) is used as a biomarker of oxidative stress because it is one of the end products of lipid peroxidation and is released by the reaction of ROS with phospholipids in cell membranes [119, 120]. The level of MDA in the cell culture medium was determined by liquid chromatography (LC) coupled to tandem mass spectrometry (MS/MS)* ***D)*** *The release of MDA was greater in SOA_{NAP}-SP than $SOA_{\beta PIN}$-SP at various dilutions.* ***E)*** *The comet assay is a sensitive technique for detecting DNA damage (single and double strand breaks) [121]. The epithelial cells and endothelial cells are harvested separately for the purpose of assessing the primary and secondary genotoxicity. Visualization of the nucleoids exposed to an electrophoretic field by fluorescence microscopy shows intact DNA in the head and damaged DNA damage in the tail of the resulting comet.* ***F)*** *Both aerosols resulted in increased primary genotoxicity, but SOA_{NAP}-SP to a greater extent. In particular, SOA_{NAP}-SP also induced increased secondary genotoxicity in endothelial cells. Figures 14A, 14C, 14D were created with BioRender.com. Figures 14B, 14D, 14F were adapted from [23].*

5.2 Bridging the Gap between Laboratory and Field Experiments

It is important to address certain limitations of the experiments discussed above. SOA_{NAP}-SP and $SOA_{\beta PIN}$-SP were obtained from a single precursor, namely NAP or βPIN. This contrasts with the high chemical diversity of aerosols in the atmosphere, which contain POA from many sources and SOA from several precursors. This is not only relevant to the atmospheric chemistry reactions that occur in the atmosphere due to interactions between SOA and other compounds in both the particulate and gas phase (also including non-organic constituents such as metals or salts) but could also influence related biological responses. Therefore, recreating realistic atmospheric conditions is a major challenge for laboratory experiments and motivates further research in real-world field settings to confirm findings from the laboratory. As such, there is a considerable need for studies bringing field and laboratory observations together.

Therefore, moving away from aerosol systems derived from individual SOA precursors, this thesis includes a case study of sugarcane biomass burning organic aerosol (BBOA) emissions from both laboratory and field experiments. As the developed TD-GC×GC-TOFMS method has proved to be particularly useful for molecular information of the particle-bound vaporizable species (see **section 5.1.3**), it was also applied to the chemical analysis of PM collected on QF filters from sugarcane combustion experiments. The evaluation included both targeted and non-targeted methods.

5.2.1 Case Study: Sugar Cane Burning in Laboratory and Field Settings

Sugar cane (*Saccharum* spp.), a major crop in tropical and subtropical areas, plays an important role in the world-wide production of food, fodder and energy [122]. Prior to harvest, excess material such as sugar cane leaves is removed in order to streamline the manual cutting of sugar cane stalks, thus optimizing harvesting and milling efficiency [123]. To achieve this, the conventional approach is to burn the sugar cane fields. This involves burning the dry parts of the plant, mainly the leaves of the sugar cane plant, leaving the moist stalk to be cut and harvested with machetes. The morphology of the sugar cane plant is shown in **Figure 15 A**. In South Africa in particular, pre-harvest burning is widespread, with around 90% of the sugar cane crop burnt [124].

In the summer of 2018, open-field burning experiments of sugar cane crops were conducted on farms in South Africa. During these experiments, a stationary measurement and sampling station was placed downwind of the field perimeter. PM was collected on QF filters. Prior to ignition, a background filter was collected to assess background levels of PM.

In addition, we conducted controlled laboratory experiments which attempted to replicate sugar cane burning by sequentially burning 150 g of dried sugar cane leaves (in five batches of 30 g each). The elemental composition, as well as the moisture content of the sugar cane leaves is provided in **Figure 15 B**. It should be noted that while the laboratory experiments used only dried sugar cane leaves as fuel, the field experiments included a significantly heterogeneous mixture of materials, including the entire sugar cane plant, neighboring vegetation, and organic entities such as insect pests, weeds

and soil biomass. Photos of the sugar cane burning experiments in the laboratory and the field are shown in **Figure 15 C**. The differences in experimental conditions, such as fuel composition, combustion dynamics and post-emission chemical processes in the atmosphere, require careful consideration when interpreting the physicochemical results.

5.2.2 Physicochemical Characterization of Sugar Cane Burning Emissions

To provide a detailed chemical fingerprint of the derived BBOA emissions from both laboratory and field experiments, we applied targeted (**Figure 15 D**) as well as non-targeted (**Figure 15 E,F**) evaluation approaches to data derived from TD–GC×GC–TOFMS measurements of PM collected on QF filters.

The targeted analysis of TD–GC×GC–TOFMS data focused on 64 typical marker compounds for biomass burning found in literature [42, 50, 123, 125-132], which were systematically grouped into eight different chemical classes. These included n-alkanes, PAHs (including oxygenated PAHs and methylated PAHs), furan derivatives, methoxyphenols, monosaccharide derivatives, phytosterols, and triterpenoids. The results are shown in **Figure 15 D**. In both laboratory experiments and field studies, a significant abundance of n-alkanes was observed, with a notable prevalence of odd-carbon n-alkanes. This characteristic odd-carbon distribution is typically associated with emissions from Gramineae plants [50]. With regard to PAHs, benzo[ghi]perylene, benzo[b]fluoranthene and benzo[e]pyrene were the most abundant compounds in the laboratory experiments. In contrast, the field experiments showed a less pronounced contribution of total PAHs to the total sum of the 64 target compounds. In particular, fluoranthene, pyrene and benzo[b]fluoranthene played a dominant role among the PAHs present in the field samples. Distinct variations in PAH emission profiles were also observed between the different sugar cane burning events in the field [123]. These distinctions were linked to factors such as weather conditions, combustion dynamics (flaming versus smoldering), biomass composition, and the partitioning of gases and particles. It is further worth highlighting that the field samples showed a notable presence of methoxyphenols, a pattern that was not replicated under laboratory conditions, except for the presence of vanillin. Methoxyphenols, derived from the pyrolysis of lignin, are well known indicators of emissions from biomass combustion [126]. Emissions of furans, resulting from the pyrolysis of hemicellulose and cellulose during both the ignition and stable combustion phases [133], were also present. Moreover, of particular interest, levoglucosan, which is a reliable marker of biomass combustion derived from the thermal decomposition of cellulose, was abundant in the field samples. Interestingly, this compound was conspicuously absent in the laboratory experiments, being replaced by its dehydrated form, levoglucosenone.

Overall, these differences in emissions between the conducted laboratory and field experiments could be attributed to differences in biomass composition, prevailing weather and combustion conditions, as well as atmospheric chemistry such as SOA formation and gas-particle partitioning.

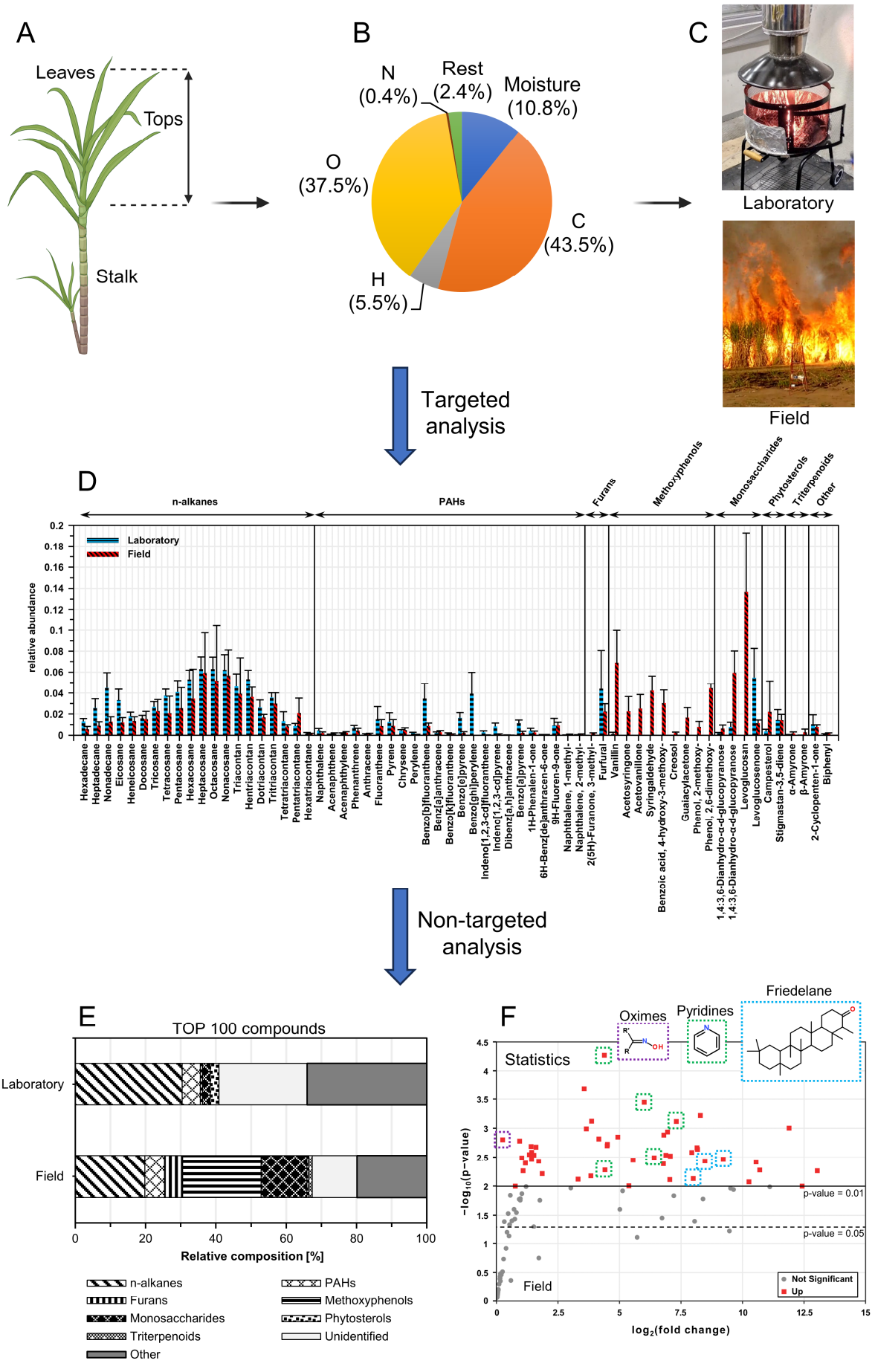

(See next page for figure description.)

Figure 15: A) *Morphology of the sugar cane plant. Created with BioRender.com.* ***B)*** *Moisture content of sugar cane leaves and elemental characterization of dried sugar cane leaves used as fuel during the laboratory experiments. Values are given in percentages by weight, % (w/w).* ***C)*** *Photograph of the combustion chamber used for the batch-wise burning of dried sugar cane leaves during the laboratory experiments (top) and of the open-field sugar cane burning experiments (bottom).* ***D)*** *Targeted analyses of 64 typical biomass burning marker compounds found in PM by TD-GC×GC-TOFMS from both the laboratory and field experiments. Each bars represents the relative total ion chromatogram (TIC) normalized area of the respective compound, with error bar corresponding to their standard deviation (laboratory: n=9; field: n=5).* ***E)*** *Non-targeted analysis of the 100 compounds with highest signal intensities found in PM of both laboratory and field experiments by TD-GC×GC-TOFMS. The bar chart features the relative abundance of different compound classes (n-alkanes, PAHs, furan derivatives, methoxyphenols, monosaccharide derivatives, phytosterols, triterpenoids and unidentified compounds).* ***F)*** *Non-targeted analysis of compounds in PM from field experiments to visualize the significance of compounds and their magnitude of changes between plume and background filters. Results are shown in a volcano plot showing only positive changes of differential abundance of chemical compounds found by TD-GC×GC-TOFMS measurements of background and stationary filters from the field campaign. Figure adapted from [134].*

Subsequently, we directed our focus towards gaining a more comprehensive understanding of the resulting BBOA emissions through the application of non-target evaluation approaches. Firstly, this was achieved by conducting a comprehensive analysis of the most abundant 100 particle-bound organic compounds from both experimental scenarios (**Figure 15 E**). Secondly, we employed a pixel-based evaluation method to statistically ascertain differences between background filter measurements and those collected within the plume during the field experiments (**Figure 15 F**).

For **Figure 15 E**, the 100 compounds with the highest signal intensities were classified into different chemical classes according to the classification for the targeted analysis (see **Figure 15 D**). In particular, the field samples contained higher proportions of monosaccharide derivatives, furans and methoxyphenols than the laboratory experiments.

Statistical analysis was performed using a Welch two-sample t-test to assess the significance of compound abundance in the sugar cane open-field burning emission plume versus background. The results were visualized in a volcano plot (**Figure 15 F**), revealing 49 compounds with positive fold changes and p-values below 0.01. Only twelve of these overlapped with the compounds shown in **Figure 15 D** (targeted analysis). This approach allowed a closer look at individual compounds associated with the pyrolysis of different bioactive compounds during sugar cane combustion.

These compounds included nitrogen-containing heteroaromatics, as well as oxime derivatives and friedelane triterpenoids. Several pyridine derivatives and quinoline, which are derived from the thermal breakdown of nitrogen-rich components in vegetation [135], were present at high fold change and significance. Given the relatively low overall nitrogen content in the sugar cane leaves of 0.4% (see **Figure 15 B**), it is imperative to incorporate compounds into chemical analysis that might only be present in minor concentrations. Moreover, an oxime derivative was also found amongst the 100 most abundant compounds both in the field and in the laboratory (refer to **Figure 15 E**) and also amongst the most significant compounds in the field (refer to **Figure 15 F**). Oximes are nitrogen-containing compounds derived from amino acids, which play a role in plant

communication, growth and development, although their functions and structures remain largely unexplored [136]. The detected oxime derivative, which could possibly be related to sugarcane burning, represents an intriguing avenue for future research and warrants further investigation. Nonetheless, the relatively low fold change (1.2) implies a minor practical impact, necessitating further validation to establish its significance. Furthermore, the identification of friedelane triterpenoids, despite their rare occurrence in plants of the Gramineae family, could point towards the possibility of their presence in the sugarcane stalks. Friedelane triterpenoids were previously detected in bamboo bark [137] and cork [138], suggesting a possible analogous distribution within the plant.

5.2.3 Complementary Perspectives from Laboratory and Field Studies

In summary, our case study of cane burning experiments in both laboratory and field settings has shown that laboratory experiments don't fully replicate real-world scenarios and capture only a subset of the insights from field experiments. While laboratory experiments provide controlled conditions, they do not capture the full organic aerosol population and complexity of real-world scenarios. Field experiments face uncontrolled variables and introduce heterogenous conditions (e.g., fuel composition, weather and combustion conditions). There are many uncertainties in field experiments, including factors such as unknown dilution rates, variations in fuel composition, and challenges in distinguishing between primary and secondary emissions. These uncertainties extend to processes such as evaporation and atmospheric ageing, which may be underway before the first samples are taken after the fire is ignited. However, because real-world situations inherently include these unpredictable elements, field studies play a critical role in assessing environmental and health impacts.

On the other hand, controlled combustion experiments in the laboratory provide information on unaltered primary marker compounds, which are crucial for source identification studies and the determination of emission factors useful for modelling studies. Thus, both laboratory and field studies are valuable and complementary. Although bridging the gap between laboratory and field results is challenging, future research will benefit from integrating these findings. Such integration could improve our understanding of biomass combustion emissions and their impacts.

Moreover, while many research studies on the chemical characterization of biomass burning emissions focus on a limited set of target compounds, such as e.g. PAHs, levoglucosan and methoxyphenols, which are indicative for biomass burning, but cannot be attributed to an individual biomass source, we demonstrated the importance of an in-depth chemical characterization through non-targeted analysis.

6 Conclusion and Outlook

Within the scope of this dissertation, we have demonstrated that aerosol science is inherently multi- and interdisciplinary, involving a combination of state-of-the-art instrumentation, laboratory experiments and field observations. This comprehensive approach has allowed us to assess the chemical complexity of organic aerosols in varying degrees of detail, ranging from overall bulk properties to detailed molecular characterization of individual compounds to characterize the wide range of multi-scale physical and chemical processes (**Figure 16**).

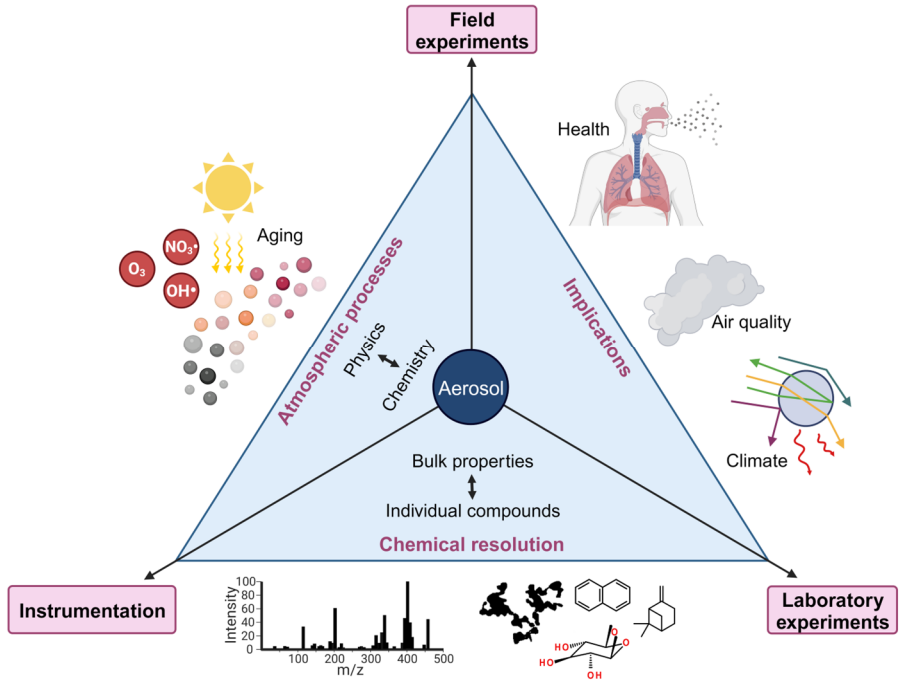

Figure 16: *Multi-disciplinary approach combining laboratory studies, field studies and state-of-the-art instrumentation with the aim to understand key processes that drive the formation and transformation of atmospheric aerosols in order to elucidate their effects on health, air quality and climate. Adapted from [139]. Created with BioRender.com.*

In this work, we demonstrated that in order to effectively address the highly diverse chemical complexity of aerosols, an intricate interplay of several instruments is required - a complex challenge for aerosol analytics. Both different aerosol types were investigated through the complementary approach of different mass spectrometric techniques. For an in-depth assessment of individual compounds at a molecular level, we demonstrated the benefit of TD–GC×GC–TOFMS, which facilitates the interpretation of the results on a molecular level due to the separation and identification of individual compounds. Thus, it allowed a selective analysis of the vaporizable aerosol compounds. Whereas in naphthalene derived SOA especially aromatic compounds (both ring-opening and ring-retaining) were detected, TD–GC×GC–TOFMS analysis revealed a high amount of predominantly cyclic and non-cyclic compounds for β-pinene derived SOA. The chemical composition of the respective aerosol could thus clearly be traced back to the chemical signatures of their respective precursor VOCs.

The *aeroHEALTH* campaign highlighted distinct biological effects on lung cells when exposed to SOA derived from both anthropogenic (naphthalene) and biogenic (β-pinene) precursors with soot as seed particles. Using a co-culture cell model, exposure to these both aerosol types revealed reduced cell viability, increased oxidative stress as well as increased primary and secondary genotoxicity. Notably, these effects were more pronounced following exposure to naphthalene derived SOA compared to β-pinene derived SOA. These observations align with the hypothesis that the toxicity of the aerosols could stem from their organic constituents. The chemical composition and oxidative properties of the produced SOA appeared to exert significant influences on the observed biological outcomes. Connecting these findings to the physicochemical characteristics of the aerosols requires a comprehensive understanding of their composition.

Furthermore, moving beyond the study of aerosol systems originating from single SOA precursors towards the integration of field and laboratory observations, another aerosol matrix originating from biomass burning (sugar cane) was studied. We found that the chemical processes during real biomass burning events can only be partially simulated by laboratory experiments. The resulting emissions, which we assessed using targeted and non-targeted approaches, included pyridine derivatives, methoxyphenols, methoxybenzenes, and triterpenoids derived from (hemi)cellulose and lignin pyrolysis. In this context, we have emphasized the value of the combination of field and laboratory approaches. While each has its own merits, field studies under real-world conditions are essential for investigations of health effects, sources, fate, or pathways of air pollutants.

In summary, this thesis contributes to understanding the relationship between the toxicological effects of aerosols and their chemical composition. Assessing the complexity of atmospheric organic aerosols requires a holistic research approach which combines laboratory and field studies with different analytical techniques. This combined approach is necessary to capture the full organic aerosol population and is of great importance for a toxicological assessment of aerosols or for investigation of their sources and reaction pathways.

However, such combined efforts in atmospheric science are just beginning to unravel the complexity of atmospheric aerosols [6]. One analytical challenge that needs to be addressed is the accurate identification and quantification of specific compounds for which there are no established standards. There's also a need for improved sampling and analytical methods to link molecular species to their adverse health effects, such as a closer look at particles deposited in the respiratory tract [10]. Ultimately, a better understanding will allow models to better predict the chemical composition of atmospheric aerosols, shedding light on how these particles affect our environment, climate, and health.

7 References

1. Sorensen, C.M., Flagan, R.C., Baltensperger, U., and Pui, D.Y.H., *Grand challenges for aerosol science and technology.* Aerosol Science and Technology, 2019. **53**(7): p. 731-734.
2. Manisalidis, I., Stavropoulou, E., Stavropoulos, A., and Bezirtzoglou, E., *Environmental and Health Impacts of Air Pollution: A Review.* Frontiers in Public Health, 2020. **8**.
3. *Health Effects Institute. State of Global Air 2020: A Special Report on Global Exposure to Air Pollution and its Health Impacts*. 2020: Boston, MA: Health Effects Institute.
4. Hallquist, M., Wenger, J.C., Baltensperger, U., Rudich, Y., Simpson, D., Claeys, M., Dommen, J., Donahue, N.M., George, C., Goldstein, A.H., Hamilton, J.F., Herrmann, H., Hoffmann, T., Iinuma, Y., Jang, M., Jenkin, M.E., Jimenez, J.L., Kiendler-Scharr, A., Maenhaut, W., McFiggans, G., Mentel, T.F., Monod, A., Prévôt, A.S.H., Seinfeld, J.H., Surratt, J.D., Szmigielski, R., and Wildt, J., *The formation, properties and impact of secondary organic aerosol: current and emerging issues.* Atmos. Chem. Phys., 2009. **9**(14): p. 5155-5236.
5. Isaacman-VanWertz, G., Massoli, P., O'Brien, R.E., Nowak, J.B., Canagaratna, M.R., Jayne, J.T., Worsnop, D.R., Su, L., Knopf, D.A., Misztal, P.K., Arata, C., Goldstein, A.H., and Kroll, J.H., *Using advanced mass spectrometry techniques to fully characterize atmospheric organic carbon: current capabilities and remaining gaps.* Faraday Discussions, 2017. **200**(0): p. 579-598.
6. Prather, K.A., Hatch, C.D., and Grassian, V.H., *Analysis of Atmospheric Aerosols.* Annual Review of Analytical Chemistry, 2008. **1**(1): p. 485-514.
7. Calvo, A.I., Alves, C., Castro, A., Pont, V., Vicente, A.M., and Fraile, R., *Research on aerosol sources and chemical composition: Past, current and emerging issues.* Atmospheric Research, 2013. **120-121**: p. 1-28.
8. World Health, O., *WHO global air quality guidelines: particulate matter (PM2.5 and PM10), ozone, nitrogen dioxide, sulfur dioxide and carbon monoxide*. 2021, Geneva: World Health Organization.
9. Boucher, O., *Atmospheric Aerosols*, in *Atmospheric Aerosols: Properties and Climate Impacts*. 2015, Springer Netherlands: Dordrecht. p. 9-24.
10. Johnston, M.V. and Kerecman, D.E., *Molecular Characterization of Atmospheric Organic Aerosol by Mass Spectrometry.* Annual Review of Analytical Chemistry, 2019. **12**(1): p. 247-274.
11. Almetwally, A.A., Bin-Jumah, M., and Allam, A.A., *Ambient air pollution and its influence on human health and welfare: an overview.* Environmental Science and Pollution Research, 2020. **27**(20): p. 24815-24830.
12. Turner, M.C., Andersen, Z.J., Baccarelli, A., Diver, W.R., Gapstur, S.M., Pope III, C.A., Prada, D., Samet, J., Thurston, G., and Cohen, A., *Outdoor air pollution and cancer: An overview of the current evidence and public health recommendations.* CA: A Cancer Journal for Clinicians, 2020. **70**(6): p. 460-479.
13. Andreae, M.O. and Crutzen, P.J., *Atmospheric Aerosols: Biogeochemical Sources and Role in Atmospheric Chemistry.* Science, 1997. **276**(5315): p. 1052-1058.
14. Mushtaq, Z., Sharma, M., Bangotra, P., Gautam, A.S., and Gautam, S., *Atmospheric Aerosols: Some Highlights and Highlighters, Past to Recent Years.* Aerosol Science and Engineering, 2022. **6**(2): p. 135-145.
15. Pacyna, J.M., *Atmospheric Deposition*, in *Encyclopedia of Ecology*, Jørgensen, S.E. and Fath, B.D., Editors. 2008, Academic Press: Oxford. p. 275-285.
16. Kwon, H.-S., Ryu, M.H., and Carlsten, C., *Ultrafine particles: unique physicochemical properties relevant to health and disease.* Experimental & Molecular Medicine, 2020. **52**(3): p. 318-328.
17. Pöschl, U., *Atmospheric Aerosols: Composition, Transformation, Climate and Health Effects.* Angewandte Chemie International Edition, 2005. **44**(46): p. 7520-7540.

18. Jimenez, J.L., Canagaratna, M.R., Donahue, N.M., Prevot, A.S.H., Zhang, Q., Kroll, J.H., DeCarlo, P.F., Allan, J.D., Coe, H., Ng, N.L., Aiken, A.C., Docherty, K.S., Ulbrich, I.M., Grieshop, A.P., Robinson, A.L., Duplissy, J., Smith, J.D., Wilson, K.R., Lanz, V.A., Hueglin, C., Sun, Y.L., Tian, J., Laaksonen, A., Raatikainen, T., Rautiainen, J., Vaattovaara, P., Ehn, M., Kulmala, M., Tomlinson, J.M., Collins, D.R., Cubison, M.J., E., Dunlea, J., Huffman, J.A., Onasch, T.B., Alfarra, M.R., Williams, P.I., Bower, K., Kondo, Y., Schneider, J., Drewnick, F., Borrmann, S., Weimer, S., Demerjian, K., Salcedo, D., Cottrell, L., Griffin, R., Takami, A., Miyoshi, T., Hatakeyama, S., Shimono, A., Sun, J.Y., Zhang, Y.M., Dzepina, K., Kimmel, J.R., Sueper, D., Jayne, J.T., Herndon, S.C., Trimborn, A.M., Williams, L.R., Wood, E.C., Middlebrook, A.M., Kolb, C.E., Baltensperger, U., and Worsnop, D.R., *Evolution of Organic Aerosols in the Atmosphere.* Science, 2009. **326**(5959): p. 1525-1529.
19. Wu, C., Wu, D., and Yu, J.Z., *Estimation and Uncertainty Analysis of Secondary Organic Carbon Using 1 Year of Hourly Organic and Elemental Carbon Data.* Journal of Geophysical Research: Atmospheres, 2019. **124**(5): p. 2774-2795.
20. Ehn, M., Thornton, J.A., Kleist, E., Sipilä, M., Junninen, H., Pullinen, I., Springer, M., Rubach, F., Tillmann, R., Lee, B., Lopez-Hilfiker, F., Andres, S., Acir, I.-H., Rissanen, M., Jokinen, T., Schobesberger, S., Kangasluoma, J., Kontkanen, J., Nieminen, T., Kurtén, T., Nielsen, L.B., Jørgensen, S., Kjaergaard, H.G., Canagaratna, M., Maso, M.D., Berndt, T., Petäjä, T., Wahner, A., Kerminen, V.-M., Kulmala, M., Worsnop, D.R., Wildt, J., and Mentel, T.F., *A large source of low-volatility secondary organic aerosol.* Nature, 2014. **506**(7489): p. 476-479.
21. Kroll, J.H., Smith, J.D., Che, D.L., Kessler, S.H., Worsnop, D.R., and Wilson, K.R., *Measurement of fragmentation and functionalization pathways in the heterogeneous oxidation of oxidized organic aerosol.* Physical Chemistry Chemical Physics, 2009. **11**(36): p. 8005-8014.
22. Kroll, J.H., Donahue, N.M., Jimenez, J.L., Kessler, S.H., Canagaratna, M.R., Wilson, K.R., Altieri, K.E., Mazzoleni, L.R., Wozniak, A.S., Bluhm, H., Mysak, E.R., Smith, J.D., Kolb, C.E., and Worsnop, D.R., *Carbon oxidation state as a metric for describing the chemistry of atmospheric organic aerosol.* Nature Chemistry, 2011. **3**(2): p. 133-139.
23. Offer, S., Hartner, E., Bucchianico, S.D., Bisig, C., Bauer, S., Pantzke, J., Zimmermann, E.J., Cao, X., Binder, S., Kuhn, E., Huber, A., Jeong, S., Käfer, U., Martens, P., Mesceriakovas, A., Bendl, J., Brejcha, R., Buchholz, A., Gat, D., Hohaus, T., Rastak, N., Jakobi, G., Kalberer, M., Kanashova, T., Hu, Y., Ogris, C., Marsico, A., Theis, F., Pardo, M., Gröger, T., Oeder, S., Orasche, J., Paul, A., Ziehm, T., Zhang, Z.-H., Adam, T., Sippula, O., Sklorz, M., Schnelle-Kreis, J., Czech, H., Kiendler-Scharr, A., Rudich, Y., and Zimmermann, R., *Effect of Atmospheric Aging on Soot Particle Toxicity in Lung Cell Models at the Air-Liquid Interface: Differential Toxicological Impacts of Biogenic and Anthropogenic Secondary Organic Aerosols (SOAs).* Environmental Health Perspectives, 2022. **130**(2): p. 027003.
24. Goldstein, A.H. and Galbally, I.E., *Known and Unexplored Organic Constituents in the Earth's Atmosphere.* Environmental Science & Technology, 2007. **41**(5): p. 1514-1521.
25. Warren, D.R. and Seinfeld, J.H., *Nucleation and Growth of Aerosol From a Continuously Reinforced Vapor.* Aerosol Science and Technology, 1984. **3**(2): p. 135-153.
26. Kurien, C., Srivastava, A.K., Gandigudi, N., and Anand, K., *Soot deposition effects and microwave regeneration modelling of diesel particulate filtration system.* Journal of the Energy Institute, 2020. **93**(2): p. 463-473.
27. Matti Maricq, M., *Chemical characterization of particulate emissions from diesel engines: A review.* Journal of Aerosol Science, 2007. **38**(11): p. 1079-1118.
28. Hamilton, J.F., Webb, P.J., Lewis, A.C., Hopkins, J.R., Smith, S., and Davy, P., *Partially oxidised organic components in urban aerosol using GCXGC-TOF/MS.* Atmos. Chem. Phys., 2004. **4**(5): p. 1279-1290.
29. Mazurek, M.A., *Molecular identification of organic compounds in atmospheric complex mixtures and relationship to atmospheric chemistry and sources.* Environmental Health Perspectives, 2002. **110**(suppl 6): p. 995-1003.

30. Lim, Y.B. and Ziemann, P.J., *Effects of Molecular Structure on Aerosol Yields from OH Radical-Initiated Reactions of Linear, Branched, and Cyclic Alkanes in the Presence of NOx.* Environmental Science & Technology, 2009. **43**(7): p. 2328-2334.
31. Shao, Y., Voliotis, A., Du, M., Wang, Y., Pereira, K., Hamilton, J., Alfarra, M.R., and McFiggans, G., *Chemical composition of secondary organic aerosol particles formed from mixtures of anthropogenic and biogenic precursors.* Atmos. Chem. Phys., 2022. **22**(15): p. 9799-9826.
32. Mahilang, M., Deb, M.K., and Pervez, S., *Biogenic secondary organic aerosols: A review on formation mechanism, analytical challenges and environmental impacts.* Chemosphere, 2021. **262**: p. 127771.
33. Laothawornkitkul, J., Taylor, J.E., Paul, N.D., and Hewitt, C.N., *Biogenic volatile organic compounds in the Earth system.* New Phytologist, 2009. **183**(1): p. 27-51.
34. Rolletter, M., Kaminski, M., Acir, I.H., Bohn, B., Dorn, H.P., Li, X., Lutz, A., Nehr, S., Rohrer, F., Tillmann, R., Wegener, R., Hofzumahaus, A., Kiendler-Scharr, A., Wahner, A., and Fuchs, H., *Investigation of the α-pinene photooxidation by OH in the atmospheric simulation chamber SAPHIR.* Atmos. Chem. Phys., 2019. **19**(18): p. 11635-11649.
35. Atkinson, R. and Arey, J., *Atmospheric Degradation of Volatile Organic Compounds.* Chemical Reviews, 2003. **103**(12): p. 4605-4638.
36. Rissanen, M., *Anthropogenic Volatile Organic Compound (AVOC) Autoxidation as a Source of Highly Oxygenated Organic Molecules (HOM).* The Journal of Physical Chemistry A, 2021. **125**(41): p. 9027-9039.
37. Atkinson, R. and Arey, J., *Atmospheric chemistry of gas-phase polycyclic aromatic hydrocarbons: formation of atmospheric mutagens.* Environmental Health Perspectives, 1994. **102**(suppl 4): p. 117-126.
38. Atkinson, R., *Atmospheric chemistry of VOCs and NOx.* Atmospheric Environment, 2000. **34**(12): p. 2063-2101.
39. Drwal, E., Rak, A., and Gregoraszczuk, E.L., *Review: Polycyclic aromatic hydrocarbons (PAHs)—Action on placental function and health risks in future life of newborns.* Toxicology, 2019. **411**: p. 133-142.
40. van der Werf, G.R., Randerson, J.T., Giglio, L., van Leeuwen, T.T., Chen, Y., Rogers, B.M., Mu, M., van Marle, M.J.E., Morton, D.C., Collatz, G.J., Yokelson, R.J., and Kasibhatla, P.S., *Global fire emissions estimates during 1997–2016.* Earth Syst. Sci. Data, 2017. **9**(2): p. 697-720.
41. Andreae, M.O. and Merlet, P., *Emission of trace gases and aerosols from biomass burning.* Global Biogeochemical Cycles, 2001. **15**(4): p. 955-966.
42. Andreae, M.O., *Emission of trace gases and aerosols from biomass burning – an updated assessment.* Atmos. Chem. Phys., 2019. **19**(13): p. 8523-8546.
43. Akagi, S.K., Yokelson, R.J., Wiedinmyer, C., Alvarado, M.J., Reid, J.S., Karl, T., Crounse, J.D., and Wennberg, P.O., *Emission factors for open and domestic biomass burning for use in atmospheric models.* Atmos. Chem. Phys., 2011. **11**(9): p. 4039-4072.
44. Yevich, R. and Logan, J.A., *An assessment of biofuel use and burning of agricultural waste in the developing world.* Global Biogeochemical Cycles, 2003. **17**(4).
45. Brandt, C.S., *Agricultural Burning.* Journal of the Air Pollution Control Association, 1966. **16**(2): p. 85-86.
46. Konovalov, I.B., Golovushkin, N.A., Beekmann, M., and Andreae, M.O., *Insights into the aging of biomass burning aerosol from satellite observations and 3D atmospheric modeling: evolution of the aerosol optical properties in Siberian wildfire plumes.* Atmos. Chem. Phys., 2021. **21**(1): p. 357-392.
47. Tayyab, M., Noman, A., Islam, W., Waheed, S., Arafat, Y., Ali, F., Zaynab, M., Lin, S., Zhang, H., and Khan, D., *Bioethanol production from lignocellulosic biomass by environment-friendly pretreatment methods: A review.* APPLIED ECOLOGY AND ENVIRONMENTAL RESEARCH, 2017. **16**.
48. Hodgson-Kratky, K., Papa, G., Rodriguez, A., Stavila, V., Simmons, B., Botha, F., Furtado, A., and Henry, R., *Relationship between sugarcane culm and leaf biomass*

composition and saccharification efficiency. Biotechnology for Biofuels, 2019. **12**(1): p. 247.

49. Khaire, K.C., Moholkar, V.S., and Goyal, A., *Bioconversion of sugarcane tops to bioethanol and other value added products: An overview.* Materials Science for Energy Technologies, 2021. **4**: p. 54-68.
50. Simoneit, B.R.T., *Biomass burning — a review of organic tracers for smoke from incomplete combustion.* Applied Geochemistry, 2002. **17**(3): p. 129-162.
51. Geiser, M. and Kreyling, W.G., *Deposition and biokinetics of inhaled nanoparticles.* Particle and Fibre Toxicology, 2010. **7**(1): p. 2.
52. Heyder, J., *Deposition of Inhaled Particles in the Human Respiratory Tract and Consequences for Regional Targeting in Respiratory Drug Delivery.* Proceedings of the American Thoracic Society, 2004. **1**(4): p. 315-320.
53. Li, D., Li, Y., Li, G., Zhang, Y., Li, J., and Chen, H., *Fluorescent reconstitution on deposition of PM2.5 in lung and extrapulmonary organs.* Proceedings of the National Academy of Sciences, 2019. **116**(7): p. 2488-2493.
54. Park, M., Joo, H.S., Lee, K., Jang, M., Kim, S.D., Kim, I., Borlaza, L.J.S., Lim, H., Shin, H., Chung, K.H., Choi, Y.-H., Park, S.G., Bae, M.-S., Lee, J., Song, H., and Park, K., *Differential toxicities of fine particulate matters from various sources.* Scientific Reports, 2018. **8**(1): p. 17007.
55. Smith, D.M., Fiddler, M.N., Pokhrel, R.P., and Bililign, S., *Laboratory studies of fresh and aged biomass burning aerosol emitted from east African biomass fuels – Part 1: Optical properties.* Atmos. Chem. Phys., 2020. **20**(17): p. 10149-10168.
56. Burling, I.R., Yokelson, R.J., Griffith, D.W.T., Johnson, T.J., Veres, P., Roberts, J.M., Warneke, C., Urbanski, S.P., Reardon, J., Weise, D.R., Hao, W.M., and de Gouw, J., *Laboratory measurements of trace gas emissions from biomass burning of fuel types from the southeastern and southwestern United States.* Atmos. Chem. Phys., 2010. **10**(22): p. 11115-11130.
57. Hodshire, A.L., Akherati, A., Alvarado, M.J., Brown-Steiner, B., Jathar, S.H., Jimenez, J.L., Kreidenweis, S.M., Lonsdale, C.R., Onasch, T.B., Ortega, A.M., and Pierce, J.R., *Aging Effects on Biomass Burning Aerosol Mass and Composition: A Critical Review of Field and Laboratory Studies.* Environmental Science & Technology, 2019. **53**(17): p. 10007-10022.
58. Bruns, E.A., El Haddad, I., Keller, A., Klein, F., Kumar, N.K., Pieber, S.M., Corbin, J.C., Slowik, J.G., Brune, W.H., Baltensperger, U., and Prévôt, A.S.H., *Inter-comparison of laboratory smog chamber and flow reactor systems on organic aerosol yield and composition.* Atmos. Meas. Tech., 2015. **8**(6): p. 2315-2332.
59. Kang, E., Root, M., Toohey, D., and Brune, W., *Introducing the concept of Potential Aerosol Mass (PAM).* Atmospheric Chemistry and Physics, 2007. **7**.
60. Rudich, Y., Donahue, N.M., and Mentel, T.F., *Aging of Organic Aerosol: Bridging the Gap Between Laboratory and Field Studies.* Annual Review of Physical Chemistry, 2007. **58**(1): p. 321-352.
61. Pardo, M., Offer, S., Hartner, E., Di Bucchianico, S., Bisig, C., Bauer, S., Pantzke, J., Zimmermann, E.J., Cao, X., Binder, S., Kuhn, E., Huber, A., Jeong, S., Käfer, U., Schneider, E., Mesceriakovas, A., Bendl, J., Brejcha, R., Buchholz, A., Gat, D., Hohaus, T., Rastak, N., Karg, E., Jakobi, G., Kalberer, M., Kanashova, T., Hu, Y., Ogris, C., Marsico, A., Theis, F., Shalit, T., Gröger, T., Rüger, C.P., Oeder, S., Orasche, J., Paul, A., Ziehm, T., Zhang, Z.-H., Adam, T., Sippula, O., Sklorz, M., Schnelle-Kreis, J., Czech, H., Kiendler-Scharr, A., Zimmermann, R., and Rudich, Y., *Exposure to naphthalene and β-pinene-derived secondary organic aerosol induced divergent changes in transcript levels of BEAS-2B cells.* Environment International, 2022. **166**: p. 107366.
62. Streibel, T., Schnelle-Kreis, J., Czech, H., Harndorf, H., Jakobi, G., Jokiniemi, J., Karg, E., Lintelmann, J., Matuschek, G., Michalke, B., Müller, L., Orasche, J., Passig, J., Radischat, C., Rabe, R., Reda, A., Rüger, C., Schwemer, T., Sippula, O., Stengel, B., Sklorz, M., Torvela, T., Weggler, B., and Zimmermann, R., *Aerosol emissions of a ship diesel engine*

operated with diesel fuel or heavy fuel oil. Environmental Science and Pollution Research, 2017. **24**(12): p. 10976-10991.
63. Reinhardt, A., Emmenegger, C., Gerrits, B., Panse, C., Dommen, J., Baltensperger, U., Zenobi, R., and Kalberer, M., *Ultrahigh Mass Resolution and Accurate Mass Measurements as a Tool To Characterize Oligomers in Secondary Organic Aerosols.* Analytical Chemistry, 2007. **79**(11): p. 4074-4082.
64. Käfer, U., Gröger, T., Rüger, C.P., Czech, H., Saraji-Bozorgzad, M., Wilharm, T., and Zimmermann, R., *Direct inlet probe – High-resolution time-of-flight mass spectrometry as fast technique for the chemical description of complex high-boiling samples.* Talanta, 2019. **202**: p. 308-316.
65. Schuetzle, D., Crittenden, A.L., and Charlson, R.J., *Application of Computer Controlled High Resolution Mass Spectrometry to the Analysis of Air Pollutants.* Journal of the Air Pollution Control Association, 1973. **23**(8): p. 704-709.
66. Canagaratna, M.R., Jayne, J.T., Jimenez, J.L., Allan, J.D., Alfarra, M.R., Zhang, Q., Onasch, T.B., Drewnick, F., Coe, H., Middlebrook, A., Delia, A., Williams, L.R., Trimborn, A.M., Northway, M.J., DeCarlo, P.F., Kolb, C.E., Davidovits, P., and Worsnop, D.R., *Chemical and microphysical characterization of ambient aerosols with the aerodyne aerosol mass spectrometer.* Mass Spectrometry Reviews, 2007. **26**(2): p. 185-222.
67. DeCarlo, P.F., Kimmel, J.R., Trimborn, A., Northway, M.J., Jayne, J.T., Aiken, A.C., Gonin, M., Fuhrer, K., Horvath, T., Docherty, K.S., Worsnop, D.R., and Jimenez, J.L., *Field-Deployable, High-Resolution, Time-of-Flight Aerosol Mass Spectrometer.* Analytical Chemistry, 2006. **78**(24): p. 8281-8289.
68. Canagaratna, M.R., Jimenez, J.L., Kroll, J.H., Chen, Q., Kessler, S.H., Massoli, P., Hildebrandt Ruiz, L., Fortner, E., Williams, L.R., Wilson, K.R., Surratt, J.D., Donahue, N.M., Jayne, J.T., and Worsnop, D.R., *Elemental ratio measurements of organic compounds using aerosol mass spectrometry: characterization, improved calibration, and implications.* Atmos. Chem. Phys., 2015. **15**(1): p. 253-272.
69. Passig, J. and Zimmermann, R., *Laser Ionization in Single-Particle Mass Spectrometry*, in *Photoionization and Photo-Induced Processes in Mass Spectrometry*. 2021. p. 359-411.
70. Li, C., He, Q., Schade, J., Passig, J., Zimmermann, R., Meidan, D., Laskin, A., and Rudich, Y., *Dynamic changes in optical and chemical properties of tar ball aerosols by atmospheric photochemical aging.* Atmos. Chem. Phys., 2019. **19**(1): p. 139-163.
71. Kari, E., Miettinen, P., Yli-Pirilä, P., Virtanen, A., and Faiola, C.L., *PTR-ToF-MS product ion distributions and humidity-dependence of biogenic volatile organic compounds.* International Journal of Mass Spectrometry, 2018. **430**: p. 87-97.
72. Lindinger, W. and Jordan, A., *Proton-transfer-reaction mass spectrometry (PTR–MS): on-line monitoring of volatile organic compounds at pptv levels.* Chemical Society Reviews, 1998. **27**(5): p. 347-375.
73. Hanley, L. and Zimmermann, R., *Light and Molecular Ions: The Emergence of Vacuum UV Single-Photon Ionization in MS.* Analytical Chemistry, 2009. **81**(11): p. 4174-4182.
74. Galvão, E.S., Santos, J.M., Lima, A.T., Reis, N.C., Orlando, M.T.D.A., and Stuetz, R.M., *Trends in analytical techniques applied to particulate matter characterization: A critical review of fundaments and applications.* Chemosphere, 2018. **199**: p. 546-568.
75. Kulkarni, P., Baron, P.A., and Willeke, K., *Introduction to Aerosol Characterization*, in *Aerosol Measurement*. 2011. p. 1-13.
76. Vallero, D.A., *Chapter 11 - Sampling and analysis*, in *Air Pollution Calculations*, Vallero, D.A., Editor. 2019, Elsevier. p. 263-333.
77. Raynor, P.C., Leith, D., Lee, K.W., and Mukund, R., *Sampling and Analysis Using Filters*, in *Aerosol Measurement*. 2011. p. 107-128.
78. Turpin, B.J., Huntzicker, J.J., and Hering, S.V., *Investigation of organic aerosol sampling artifacts in the los angeles basin.* Atmospheric Environment, 1994. **28**(19): p. 3061-3071.
79. Hartner, E., Paul, A., Käfer, U., Czech, H., Hohaus, T., Gröger, T., Sklorz, M., Jakobi, G., Orasche, J., Jeong, S., Brejcha, R., Ziehm, T., Zhang, Z.-H., Schnelle-Kreis, J., Adam, T., Rudich, Y., Kiendler-Scharr, A., and Zimmermann, R., *On the Complementarity and Informative Value of Different Electron Ionization Mass Spectrometric Techniques for the*

Chemical Analysis of Secondary Organic Aerosols. ACS Earth and Space Chemistry, 2022. **6**(5): p. 1358-1374.

80. Zhang, Z.H., Hartner, E., Utinger, B., Gfeller, B., Paul, A., Sklorz, M., Czech, H., Yang, B.X., Su, X.Y., Jakobi, G., Orasche, J., Schnelle-Kreis, J., Jeong, S., Gröger, T., Pardo, M., Hohaus, T., Adam, T., Kiendler-Scharr, A., Rudich, Y., Zimmermann, R., and Kalberer, M., *Are reactive oxygen species (ROS) a suitable metric to predict toxicity of carbonaceous aerosol particles?* Atmos. Chem. Phys., 2022. **22**(3): p. 1793-1809.
81. Wang, S., Kuo, Y.-M., Lin, C.-W., Huang, S.-H., Fu, B., Zhang, Q., and Chen, C.-C., *A Simple Method for Aerosol Transport Efficiency Tests in Sampling Tubes.* Aerosol and Air Quality Research, 2022. **22**(11): p. 220219.
82. Gross, J.H., *Introduction*, in *Mass Spectrometry: A Textbook*. 2017, Springer International Publishing: Cham. p. 1-28.
83. Eljarrat, E. and Barceló, D., *MASS SPECTROMETRY | Electron Impact and Chemical Ionization*, in *Encyclopedia of Analytical Science (Second Edition)*, Worsfold, P., Townshend, A., and Poole, C., Editors. 2005, Elsevier: Oxford. p. 359-366.
84. Gross, J.H., *Principles of Ionization and Ion Dissociation*, in *Mass Spectrometry: A Textbook*. 2017, Springer International Publishing: Cham. p. 29-84.
85. Parshintsev, J. and Hyötyläinen, T., *Methods for characterization of organic compounds in atmospheric aerosol particles.* Analytical and Bioanalytical Chemistry, 2015. **407**(20): p. 5877-5897.
86. Kind, T. and Fiehn, O., *Advances in structure elucidation of small molecules using mass spectrometry.* Bioanalytical reviews, 2010. **2**(1-4): p. 23-60.
87. Gross, J.H., *Instrumentation*, in *Mass Spectrometry: A Textbook*. 2017, Springer International Publishing: Cham. p. 151-292.
88. Rockwood, A.L., Kushnir, M.M., and Clarke, N.J., *2 - Mass Spectrometry*, in *Principles and Applications of Clinical Mass Spectrometry*, Rifai, N., Horvath, A.R., and Wittwer, C.T., Editors. 2018, Elsevier. p. 33-65.
89. Yavor, M., Verentchikov, A., Hasin, J., Kozlov, B., Gavrik, M., and Trufanov, A., *Planar multi-reflecting time-of-flight mass analyzer with a jig-saw ion path.* Physics Procedia, 2008. **1**(1): p. 391-400.
90. Byer, J.D., Siek, K., and Jobst, K., *Distinguishing the C3 vs SH4 Mass Split by Comprehensive Two-Dimensional Gas Chromatography–High Resolution Time-of-Flight Mass Spectrometry.* Analytical Chemistry, 2016. **88**(12): p. 6101-6104.
91. Gröger, T.M., Käfer, U., and Zimmermann, R., *Gas chromatography in combination with fast high-resolution time-of-flight mass spectrometry: Technical overview and perspectives for data visualization.* TrAC Trends in Analytical Chemistry, 2020. **122**: p. 115677.
92. Drewnick, F., Hings, S.S., DeCarlo, P., Jayne, J.T., Gonin, M., Fuhrer, K., Weimer, S., Jimenez, J.L., Demerjian, K.L., Borrmann, S., and Worsnop, D.R., *A New Time-of-Flight Aerosol Mass Spectrometer (TOF-AMS)—Instrument Description and First Field Deployment.* Aerosol Science and Technology, 2005. **39**(7): p. 637-658.
93. Nash, D.G., Baer, T., and Johnston, M.V., *Aerosol mass spectrometry: An introductory review.* International Journal of Mass Spectrometry, 2006. **258**(1): p. 2-12.
94. Jayne, J., Leard, D., Zhang, X., Davidovcits, P., Smith, K., Kolb, C., and Worsnop, D., *Development of an Aerosol Mass Spectrometer for Size and Composition Analysis of Submicron Particles.* Aerosol Science and Technology, 2000. **33**: p. 49-70.
95. Flego, C., Carati, C., Gaudio, L.D., and Zannoni, C., *Direct Mass Spectrometry of tar sands: A new approach to bitumen identification.* Fuel, 2013. **111**: p. 357-366.
96. Cordero, C., Liberto, E., Bicchi, C., Rubiolo, P., Reichenbach, S.E., Tian, X., and Tao, Q., *Targeted and Non-Targeted Approaches for Complex Natural Sample Profiling by GC×GC-qMS.* Journal of Chromatographic Science, 2010. **48**(4): p. 251-261.
97. Reichenbach, S.E., Tian, X., Cordero, C., and Tao, Q., *Features for non-targeted cross-sample analysis with comprehensive two-dimensional chromatography.* J Chromatogr A, 2012. **1226**: p. 140-8.
98. Barmet, P., Dommen, J., DeCarlo, P.F., Tritscher, T., Praplan, A.P., Platt, S.M., Prévôt, A.S.H., Donahue, N.M., and Baltensperger, U., *OH clock determination by proton transfer*

reaction mass spectrometry at an environmental chamber. Atmos. Meas. Tech., 2012. **5**(3): p. 647-656.

99. Wragg, F.P.H., Fuller, S.J., Freshwater, R., Green, D.C., Kelly, F.J., and Kalberer, M., *An automated online instrument to quantify aerosol-bound reactive oxygen species (ROS) for ambient measurement and health-relevant aerosol studies.* Atmos. Meas. Tech., 2016. **9**(10): p. 4891-4900.
100. Fuller, S.J., Wragg, F.P.H., Nutter, J., and Kalberer, M., *Comparison of on-line and off-line methods to quantify reactive oxygen species (ROS) in atmospheric aerosols.* Atmospheric Environment, 2014. **92**: p. 97-103.
101. Chowdhury, P.H., He, Q., Lasitza Male, T., Brune, W.H., Rudich, Y., and Pardo, M., *Exposure of Lung Epithelial Cells to Photochemically Aged Secondary Organic Aerosol Shows Increased Toxic Effects.* Environmental Science & Technology Letters, 2018. **5**(7): p. 424-430.
102. Zhang, Q., Jimenez, J.L., Canagaratna, M.R., Ulbrich, I.M., Ng, N.L., Worsnop, D.R., and Sun, Y., *Understanding atmospheric organic aerosols via factor analysis of aerosol mass spectrometry: a review.* Analytical and Bioanalytical Chemistry, 2011. **401**(10): p. 3045-3067.
103. Liu, P.S.K., Deng, R., Smith, K.A., Williams, L.R., Jayne, J.T., Canagaratna, M.R., Moore, K., Onasch, T.B., Worsnop, D.R., and Deshler, T., *Transmission Efficiency of an Aerodynamic Focusing Lens System: Comparison of Model Calculations and Laboratory Measurements for the Aerodyne Aerosol Mass Spectrometer.* Aerosol Science and Technology, 2007. **41**(8): p. 721-733.
104. Aiken, A.C., DeCarlo, P.F., Kroll, J.H., Worsnop, D.R., Huffman, J.A., Docherty, K.S., Ulbrich, I.M., Mohr, C., Kimmel, J.R., Sueper, D., Sun, Y., Zhang, Q., Trimborn, A., Northway, M., Ziemann, P.J., Canagaratna, M.R., Onasch, T.B., Alfarra, M.R., Prevot, A.S.H., Dommen, J., Duplissy, J., Metzger, A., Baltensperger, U., and Jimenez, J.L., *O/C and OM/OC Ratios of Primary, Secondary, and Ambient Organic Aerosols with High-Resolution Time-of-Flight Aerosol Mass Spectrometry.* Environmental Science & Technology, 2008. **42**(12): p. 4478-4485.
105. Corbin, J.C., Othman, A., Allan, J.D., Worsnop, D.R., Haskins, J.D., Sierau, B., Lohmann, U., and Mensah, A.A., *Peak-fitting and integration imprecision in the Aerodyne aerosol mass spectrometer: effects of mass accuracy on location-constrained fits.* Atmos. Meas. Tech., 2015. **8**(11): p. 4615-4636.
106. Ahn, Y.G., Jeon, S.H., Lim, H.B., Choi, N.R., Hwang, G.-S., Kim, Y.P., and Lee, J.Y., *Analysis of Polycyclic Aromatic Hydrocarbons in Ambient Aerosols by Using One-Dimensional and Comprehensive Two-Dimensional Gas Chromatography Combined with Mass Spectrometric Method: A Comparative Study %J Journal of Analytical Methods in Chemistry.* Journal of Analytical Methods in Chemistry, 2018. **2018**: p. 9.
107. Maceira, A., Marcé, R.M., and Borrull, F., *Analytical methods for determining organic compounds present in the particulate matter from outdoor air.* TrAC Trends in Analytical Chemistry, 2020. **122**: p. 115707.
108. Chow, J.C., Watson, J.G., Chen, L.W.A., Chang, M.C.O., Robinson, N.F., Trimble, D., and Kohl, S., *The IMPROVE_A Temperature Protocol for Thermal/Optical Carbon Analysis: Maintaining Consistency with a Long-Term Database.* Journal of the Air & Waste Management Association, 2007. **57**(9): p. 1014-1023.
109. Shiroudi, A., Deleuze, M.S., and Canneaux, S., *Theoretical Study of the Oxidation Mechanisms of Naphthalene Initiated by Hydroxyl Radicals: The OH-Addition Pathway.* The Journal of Physical Chemistry A, 2014. **118**(26): p. 4593-4610.
110. Keyte, I.J., Harrison, R.M., and Lammel, G., *Chemical reactivity and long-range transport potential of polycyclic aromatic hydrocarbons – a review.* Chemical Society Reviews, 2013. **42**(24): p. 9333-9391.
111. Sasaki, J., Aschmann, S.M., Kwok, E.S.C., Atkinson, R., and Arey, J., *Products of the Gas-Phase OH and NO3 Radical-Initiated Reactions of Naphthalene.* Environmental Science & Technology, 1997. **31**(11): p. 3173-3179.

112. Sato, K., Jia, T., Tanabe, K., Morino, Y., Kajii, Y., and Imamura, T., *Terpenylic acid and nine-carbon multifunctional compounds formed during the aging of β-pinene ozonolysis secondary organic aerosol.* Atmospheric Environment, 2016. **130**: p. 127-135.
113. Karg, E.W., Ferron, G.A., Bauer, S., Di Bucchianico, S., and Zimmermann, R., *Is the particle deposition in a cell exposure facility comparable to the lungs? A computer model approach.* Aerosol Science and Technology, 2020. **54**(6): p. 668-684.
114. Al-Kindi, S.G., Brook, R.D., Biswal, S., and Rajagopalan, S., *Environmental determinants of cardiovascular disease: lessons learned from air pollution.* Nature Reviews Cardiology, 2020. **17**(10): p. 656-672.
115. Liu, F., Saavedra, M.G., Champion, J.A., Griendling, K.K., and Ng, N.L., *Prominent Contribution of Hydrogen Peroxide to Intracellular Reactive Oxygen Species Generated upon Exposure to Naphthalene Secondary Organic Aerosols.* Environmental Science & Technology Letters, 2020. **7**(3): p. 171-177.
116. Gopinath, P., Mahammed, A., Ohayon, S., Gross, Z., and Brik, A., *Understanding and predicting the potency of ROS-based enzyme inhibitors, exemplified by naphthoquinones and ubiquitin specific protease-2.* Chemical Science, 2016. **7**(12): p. 7079-7086.
117. Chan, F.K.-M., Moriwaki, K., and De Rosa, M.J., *Detection of Necrosis by Release of Lactate Dehydrogenase Activity*, in *Immune Homeostasis: Methods and Protocols*, Snow, A.L. and Lenardo, M.J., Editors. 2013, Humana Press: Totowa, NJ. p. 65-70.
118. Kumar, P., Nagarajan, A., and Uchil, P.D., *Analysis of Cell Viability by the Lactate Dehydrogenase Assay.* Cold Spring Harbor Protocols, 2018. **2018**(6): p. pdb.prot095497.
119. Del Rio, D., Stewart, A.J., and Pellegrini, N., *A review of recent studies on malondialdehyde as toxic molecule and biological marker of oxidative stress.* Nutrition, Metabolism and Cardiovascular Diseases, 2005. **15**(4): p. 316-328.
120. Tsikas, D., *Assessment of lipid peroxidation by measuring malondialdehyde (MDA) and relatives in biological samples: Analytical and biological challenges.* Analytical Biochemistry, 2017. **524**: p. 13-30.
121. Di Bucchianico, S., Cappellini, F., Le Bihanic, F., Zhang, Y., Dreij, K., and Karlsson, H.L., *Genotoxicity of TiO2 nanoparticles assessed by mini-gel comet assay and micronucleus scoring with flow cytometry.* Mutagenesis, 2016. **32**(1): p. 127-137.
122. Dinesh Babu, K.S., Janakiraman, V., Palaniswamy, H., Kasirajan, L., Gomathi, R., and Ramkumar, T.R., *A short review on sugarcane: its domestication, molecular manipulations and future perspectives.* Genetic Resources and Crop Evolution, 2022. **69**(8): p. 2623-2643.
123. Geldenhuys, G., Orasche, J., Jakobi, G., Zimmermann, R., and Forbes, P.B.C., *Characterization of Gaseous and Particulate Phase Polycyclic Aromatic Hydrocarbons Emitted During Preharvest Burning of Sugar Cane in Different Regions of Kwa-Zulu Natal, South Africa.* Environmental Toxicology and Chemistry, 2023. **42**(4): p. 778-792.
124. Pryor, S.W., Smithers, J., Lyne, P., and van Antwerpen, R., *Impact of agricultural practices on energy use and greenhouse gas emissions for South African sugarcane production.* Journal of Cleaner Production, 2017. **141**: p. 137-145.
125. Moraes, M.S.A., Georges, F., Almeida, S.R., Damasceno, F.C., Maciel, G.P.d.S., Zini, C.A., Jacques, R.A., and Caramão, E.B., *Analysis of products from pyrolysis of Brazilian sugar cane straw.* Fuel Processing Technology, 2012. **101**: p. 35-43.
126. Liu, C., Chen, D., and Chen, X.e., *Atmospheric Reactivity of Methoxyphenols: A Review.* Environmental Science & Technology, 2022. **56**(5): p. 2897-2916.
127. Li, W., Ge, P., Chen, M., Tang, J., Cao, M., Cui, Y., Hu, K., and Nie, D., *Tracers from Biomass Burning Emissions and Identification of Biomass Burning.* Atmosphere, 2021. **12**(11): p. 1401.
128. dos Santos, C.Y.M., Azevedo, D.d.A., and de Aquino Neto, F.R., *Selected organic compounds from biomass burning found in the atmospheric particulate matter over sugarcane plantation areas.* Atmospheric Environment, 2002. **36**(18): p. 3009-3019.
129. Lin, Y.-C., Cho, J., Tompsett, G.A., Westmoreland, P.R., and Huber, G.W., *Kinetics and Mechanism of Cellulose Pyrolysis.* The Journal of Physical Chemistry C, 2009. **113**(46): p. 20097-20107.

130. Worton, D.R., Goldstein, A.H., Farmer, D.K., Docherty, K.S., Jimenez, J.L., Gilman, J.B., Kuster, W.C., de Gouw, J., Williams, B.J., Kreisberg, N.M., Hering, S.V., Bench, G., McKay, M., Kristensen, K., Glasius, M., Surratt, J.D., and Seinfeld, J.H., *Origins and composition of fine atmospheric carbonaceous aerosol in the Sierra Nevada Mountains, California.* Atmos. Chem. Phys., 2011. **11**(19): p. 10219-10241.
131. Samburova, V., Connolly, J., Gyawali, M., Yatavelli, R.L.N., Watts, A.C., Chakrabarty, R.K., Zielinska, B., Moosmüller, H., and Khlystov, A., *Polycyclic aromatic hydrocarbons in biomass-burning emissions and their contribution to light absorption and aerosol toxicity.* Science of The Total Environment, 2016. **568**: p. 391-401.
132. Shen, G., Xue, M., Wei, S., Chen, Y., Wang, B., Wang, R., Lv, Y., Shen, H., Li, W., Zhang, Y., Huang, Y., Chen, H., Wei, W., Zhao, Q., Li, B., Wu, H., and Tao, S., *Emissions of parent, nitrated, and oxygenated polycyclic aromatic hydrocarbons from indoor corn straw burning in normal and controlled combustion conditions.* Journal of Environmental Sciences, 2013. **25**(10): p. 2072-2080.
133. Czech, H., Sippula, O., Kortelainen, M., Tissari, J., Radischat, C., Passig, J., Streibel, T., Jokiniemi, J., and Zimmermann, R., *On-line analysis of organic emissions from residential wood combustion with single-photon ionisation time-of-flight mass spectrometry (SPI-TOFMS).* Fuel, 2016. **177**: p. 334-342.
134. Hartner, E., Gawlitta, N., Gröger, T., Orasche, J., Czech, H., Geldenhuys, G.-L., Jakobi, G., Tiitta, P., Yli-Pirilä, P., Kortelainen, M., Sippula, O., Forbes, P.B.C., and Zimmermann, R., *Chemical Fingerprinting of Biomass Burning Organic Aerosols from Sugarcane Combustion: Complementary Findings from Field and Laboratory Studies.* Environmental Science & Technology, 2023. **(under review)**.
135. Ma, Y. and Hays, M.D., *Thermal extraction–two-dimensional gas chromatography–mass spectrometry with heart-cutting for nitrogen heterocyclics in biomass burning aerosols.* Journal of Chromatography A, 2008. **1200**(2): p. 228-234.
136. Sørensen, M., Neilson, E.H.J., and Møller, B.L., *Oximes: Unrecognized Chameleons in General and Specialized Plant Metabolism.* Molecular Plant, 2018. **11**(1): p. 95-117.
137. Radi, M.H., El-Shiekh, R.A., El-Halawany, A.M., and Abdel-Sattar, E., *Friedelin and 3β-Friedelinol: Pharmacological Activities.* Revista Brasileira de Farmacognosia, 2023.
138. Coquet, C., Ferré, E., Peyronel, D., Dal Farra, C., and Farnet, A.M., *Identification of new molecules extracted from Quercus suber L. cork.* Comptes Rendus Biologies, 2008. **331**(11): p. 853-858.
139. Su, H., Cheng, Y., and Pöschl, U., *New Multiphase Chemical Processes Influencing Atmospheric Aerosols, Air Quality, and Climate in the Anthropocene.* Accounts of Chemical Research, 2020. **53**(10): p. 2034-2043.

8 Appendix

8.1 List of Abbreviations

ALI	air-liquid interface
AMS	aerosol mass spectrometry
BBOA	biomass burning organic aerosol
BC	black carbon
BrC	brown carbon
CCN	cloud condensation nuclei
CI	chemical ionization
COPD	chronic obstructive pulmonary disease
CPC	condensation particle counter
DIP	direct inlet probe
EC	elemental carbon
EI	electron ionization
ELVOC	extremely low volatility organic compounds
ESI	electrospray ionization
FTICRMS	Fourier transform ion cyclotron resonance mass spectrometry
GC	gas chromatography
GC×GC	comprehensive two-dimensional gas chromatography
H/C	hydrogen-to-carbon ratio
HR	high-resolution
HRTOFMS	high-resolution time-of-flight mass spectrometry
IR	infrared
LC	liquid chromatography
LDH	lactate dehydrogenase
m/z	mass-to-charge ratio
MDA	malondialdehyde
mini-CAST	miniature combustion aerosol standard
MS	mass spectrometry
MS/MS	tandem mass spectrometry
MS-mode	mass spectrum mode (AMS)
NAP	naphthalene
NIST	US National Institute of Standards and Technology
NMR	nuclear magnetic resonance
O/C	oxygen-to-carbon ratio
OA	organic aerosol
OC	organic carbon
OFR	oxidation flow reactor
OPROSI	particle-bound ROS instrument
OS_C	carbon oxidation state
PAH	polycyclic aromatic hydrocarbon
PAM	potential aerosol mass
PI	photoionization
PIMS	photoionization mass spectrometry

PM	particulate matter
POA	primary organic aerosol
PTOF-mode	particle time-of-flight mode (AMS)
PTR-MS	proton-transfer-reaction mass spectrometer
QF	quartz fiber
ROS	reactive oxygen species
SMPS	scanning mobility particle sizer
SOA	secondary organic aerosol
SOA_{NAP}-SP	secondary organic aerosols derived from photooxidation of naphthalene as precursor and soot as seed particles
$SOA_{\beta PIN}$-SP	secondary organic aerosols derived from photooxidation of β-pinene as precursor and soot as seed particles
SP	soot particle
SPMS	single particle mass spectrometer
TD	thermal desorption
TEM	transmission electron microscopy
TOF	time-of-flight
UFP	ultrafine particles
VOC	volatile organic compound
v_p	vapor pressure
WHO	World Health Organization
βPIN	β-pinene

8.2 List of Figures

8.3 List of Tables

8.4 Publications (only in printed version)

Publication 1:

Hartner, E.; Paul, A.; Käfer, U.; Czech, H.; Hohaus, T.; Gröger, T.; Sklorz, M.; Jakobi, G.; Orasche, J.; Jeong, S.; Brejcha, R.; Ziehm, T.; Zhang, Z.-H.; Schnelle-Kreis, J.; Adam, T.; Rudich, Y.; Kiendler-Scharr, A.; Zimmermann, R., On the Complementarity and Informative Value of Different Electron Ionization Mass Spectrometric Techniques for the Chemical Analysis of Secondary Organic Aerosols. *ACS Earth and Space Chemistry* 2022, *6* (5), 1358-1374. DOI: 10.1021/acsearthspacechem.2c00039

Publication 2

Offer, S.; **Hartner, E.**; Bucchianico, S. D.; Bisig, C.; Bauer, S.; Pantzke, J.; Zimmermann, E. J.; Cao, X.; Binder, S.; Kuhn, E.; Huber, A.; Jeong, S.; Käfer, U.; Martens, P.; Mesceriakovas, A.; Bendl, J.; Brejcha, R.; Buchholz, A.; Gat, D.; Hohaus, T.; Rastak, N.; Jakobi, G.; Kalberer, M.; Kanashova, T.; Hu, Y.; Ogris, C.; Marsico, A.; Theis, F.; Pardo, M.; Gröger, T.; Oeder, S.; Orasche, J.; Paul, A.; Ziehm, T.; Zhang, Z.-H.; Adam, T.; Sippula, O.; Sklorz, M.; Schnelle-Kreis, J.; Czech, H.; Kiendler-Scharr, A.; Rudich, Y.; Zimmermann, R., Effect of Atmospheric Aging on Soot Particle Toxicity in Lung Cell Models at the Air–Liquid Interface: Differential Toxicological Impacts of Biogenic and Anthropogenic Secondary Organic Aerosols (SOAs). *Environmental Health Perspectives* 2022, *130* (2), 027003. DOI: 10.1289/EHP9413

Publication 3 (submitted)

Hartner, E.; Gawlitta, N.; Gröger, T.; Orasche, J.; Czech, H.; Geldenhuys, G.-L.; Jakobi, G.; Titta, P.; Yli-Pirilä, P.; Kortelainen, M; Sippula, O.; Forbes, P.; Zimmermann, R., Chemical Fingerprinting of Biomass Burning Organic Aerosols from Sugar Cane Combustion: Complementary Findings from Field and Laboratory Studies. *ACS Environmental Science and Technology*, 2023 (submitted).